Met Office

A review of Stratospheric Sounding Unit radiance observations in support of climate trends investigations and reanalysis

Forecasting Research
Technical Report No: 586

December 2013

John Nash and Roger Saunders

Contents

Abstract **4**

1. Introduction **5**

2. Overview of the SSU instrument and its measurements **8**

2.1 Principles of operation of the SSU 8

2.2 History of the SSU data processing 10

2.3 SSU data reprocessing 11

3. Met Office processing from counts to calibrated radiances **12**

3.1 Prelaunch tests 12

3.2 Averaging of radiances 15

3.3 In-orbit performance 16

3.3.1 Radiometric noise 16

3.3.2 Systematic biases observed between spacecraft 18

3.4 Synthesised radiances 20

4. Spectroscopic performance of SSU **24**

4.1. Laboratory testing 24

4.2 Sensitivity of temperature weighting functions to temperature profile 26

4.3 Spectroscopic assessment after launch 28

4.4 Correction for increasing concentration of atmospheric carbon dioxide 30

5. The influence of solar tides on the SSU time series **32**

5.1 Observations of migrating solar temperature tides 32

5.2 The impact of solar tides on the time series analysis 36

6. Time series analysis **40**

6.1 Updated Met Office time series 40

6.1.1 Channel 1 details 41

6.1.2 Channel 2 details 42

6.1.3 Channel 3 details 42

6.1.4 All upper level synthetic channels 42

6.1.5 All lower level synthetic channels 44

6.1.6 Uncertainty estimates 44

6.2 Analysis of the differences between the Met Office time series and others 47

6.2.1 Modifications to the WANG, LIU and BRINDLEY and NASH time series 48

6.2.2 Data coverage 50

6.2.3 Data availability 50

6.2.4 Differences in radiometric quality 52

6.2.5 Differences in spectroscopic corrections 52

6.2.6 Differences in tidal corrections 52

7. Conclusions **53**

8. Acknowledgements **55**

Bibliography **55**

Annex 1. Timeline of SSU data **58**

Abstract

The Stratospheric Sounding Unit (SSU) on the NOAA polar orbiting satellites measured stratospheric temperatures between late 1978 and mid-2006. Emitted radiances from carbon dioxide in 3 channels centred at mean pressure levels of 9, 5 and 2 hPa, enabled continuous monitoring of the stratospheric and lower mesospheric temperature to provide a climate dataset for the middle atmosphere. Discrepancies in the temperature analyses between the original Met Office study and more recent analyses have been highlighted by Thompson et al (2012)[1]. This paper is the Met Office response to Thompson et al (2012), summarising the issues to be resolved in creating a climate data record from the different SSUs, including corrections for radiometric, spectroscopic and tidal differences. The results presented here are slightly different from the earlier published time series attributed to the Met Office in Thompson et al (2012). The origin of the differences between the Met Office time series and others is discussed in detail. The most significant source of uncertainty was found to be in the tidal correction for all channels. Calibration issues identified include the SSU space view anomaly and radiometric anomalies in the NOAA-9 observations. The analysis by Wang et al (2012) has a significantly different temperature time series for SSU channels 1 and 2 compared to the results presented here. In Wang et al (2012) the radiometric errors were not consistently corrected for the early SSUs. This resulted in the application of a merging technique with errors in the resulting fit introducing spurious temperature trends between 1979 and 1997. Correction for tidal differences is essential but these were underestimated in all channels. In a second analysis by Liu and Weng (2011) missing data and mismatches in the time series introduced errors in the analysis, and no correction for tides was applied. If these omissions are corrected the temperature changes from 1980 to 2005 become consistent within the level of uncertainty for all three analyses for SSU channels 1 and 2.

[1] Thompson, D. W. J., D. J. Seidel, W. J. Randel, C.-Z. Zou, A.H. Butler, C. Mears, A. Osso, C. Long, R. Lin, (2012) The mystery of recent stratospheric temperature trends. *Nature,* **491**, 692-697. *doi:10.1038/nature11579*

1. Introduction

Long term changes in stratospheric temperatures are important for interpreting the radiative effects of anthropogenic emissions of ozone depleting substances and greenhouse gases (e.g. Ramaswamy *et. al.*, 2001). Satellite measurements of stratospheric temperature now span more than 30 years which potentially can provide valuable information on temperature trends since 1979. Thompson *et. al.* (2012) have shown however that stratospheric temperature records inferred from the Stratospheric Sounding Unit (SSU), on the NOAA satellites, are inconsistent and this 'mystery' needs to be resolved. They recommended that one of the datasets, which originated from the Met Office, should be fully documented in the scientific literature to help identify the reasons for the differences between it and other datasets using the same satellite data but different processing methods (e.g. Wang *et. al*., 2012). This paper is a response to that request and is a comprehensive review of the generation of stratospheric temperatures from the SSU which operated between late 1978 and mid-2006.

The global climate observing system for monitoring stratospheric temperatures uses a variety of observing systems with different measurement techniques including research and operational systems. The Met Office, as part of its contribution to the Global Observing System, provided the SSU instrument to operationally monitor the stratosphere in near real time.

The SSU measurements complement those from radiosondes which can observe at high vertical resolution at all heights from the surface to about 33km[2]. However errors at upper levels in widely used radiosondes were not only present during the daytime but also in night-time measurements of many types (e.g. WMO, 2008). Improved sensor coatings and radiosonde technology has reduced the magnitude of these errors since 1984, but measurements in earlier years were usually of much poorer quality. Gravity waves with vertical wavelengths, mostly between 1 and 2 km, limit the representativeness of an individual radiosonde temperature measurement in the stratosphere (Nash *et. al*., 2006). In contrast the deep layers observed by the nadir viewing SSU radiance measurements minimise the influence of short vertical wavelength gravity waves on the satellite soundings.

[2] The data referenced here extended up to about 24 km, (Thompson and Solomon, 2005) and 30 km in Seidel et al (2005).

Layer averages of temperature in the stratosphere became available from infrared and microwave sounders mounted on TIROS-N, the first of the series of NOAA polar orbiting satellites launched in 1978. The TIROS Operational Vertical Sounder (TOVS) included:

- The Microwave Sounding Unit (MSU) observing radiances in the 50-60GHz oxygen absorption band in four channels with the highest channel peaking near 20 km. The MSU flew on all the NOAA polar orbiters up to NOAA-14.
- The Stratospheric Sounding Unit (SSU) observing radiances in the 15 micron carbon dioxide band, with three channels peaking at about 29 km, 35 km and 45 km. The designation of these channels here is 1 to 3 respectively, although they are often referred to as channels 25 to 27 of TOVS in the literature. The radiances originated from deep atmospheric layers (see section 4.2). For nadir views the half-width varies from 16 km deep (channel 1) to about 22 km (channel 3). The SSU only flew on TIROS-N and NOAA's 6, 7, 8, 9, 11 and 14, see Annex 1 for details.
- The High Resolution Infrared radiation Sounder, HIRS/2, with three channels observing in the stratosphere, but here only channel 2 was used, peaking at 20 km with a vertical resolution similar to the SSU. HIRS flew on all the NOAA polar orbiters.

In 1998, the Advanced Microwave Sounding Unit (AMSU-A) was launched on NOAA-15 with nominally six channels centred in the 50-60GHz oxygen band for temperature sensing of the stratosphere from 13 km up to 42 km. All AMSU-A channels have better vertical resolution than the SSU observations, and their measurements became the primary operational measurement of stratospheric temperatures from 1998. Collection of data from the last SSU on NOAA-14 was terminated in 2006.

A newer instrument, the Special Sensor Microwave Imager (SSMIS) launched in 2003 includes channels at 60GHz which can sound well into the mesosphere up to 80 km and is now being used in operational forecasting models (Yan and Weng, 2012). Finally the latest contribution to the stratospheric temperature record is the constellation of GPS Radio Occultation measurements which have been available since 2000. These provide temperature profiles, averaged in the horizontal, in the range from 5-40 km (e.g. Healy *et. al.* (2007) and Gleisner and Healy (2013)) depending on the atmospheric state.

Early satellite measurements of the stratosphere, before the SSU, were made by the B channels of the Selective Chopper Radiometer on Nimbus-5, Ellis *et. al.* (1973) which observed at similar heights to the SSU during 1973 and 1974. The Pressure Modulator

Radiometer on Nimbus-6 (Curtis *et. al.*, 1974) observed at heights from 45 to 85km from July 1975 until June 1978. These data cannot be linked directly to the SSU observations, but were incorporated in the CIRA-86 reference atmosphere (Fleming *et. al.,* 1990) and may be used in future reanalyses.

During the early years of the SSU the temperature retrievals were primarily used by centres involved in real-time monitoring of the stratosphere (Pick and Brownscombe, 1981, Bailey *et. al.,* 1993). More recently, as the record has reached over 25 years, interest has moved to using the measurements for monitoring stratospheric climate trends both as an independent dataset and for assimilation in reanalyses. The time series of radiances from the Met Office SSU monitoring was initially documented in Nash and Forrester (1986) and Nash and Edge (1989) and up to 1995 it was provided to Ramaswamy *et al* (2005). Shine *et al* (2008) estimated the effect of the increase in atmospheric carbon dioxide on the time series up to 1997. The full time series to 2006 was included in Randel *et. al.* (2009) with an overall drop in brightness temperature between 1979/80 and 2004/5 reported of 1.2 K in channel 1. Seidel *et. al.* (2011) included results from Liu and Weng (2009) (hereafter referred to as LIU) for SSU channels 1 and 2 where, global temperature between 1979/80 and 2004/5 fell by 1.7 K for channel 1. Wang *et. al.* (2012) (hereafter referred to as WANG) analysed SSU data from the NOAA Comprehensive Large Array data Stewardship System (CLASS) archive finding a drop in global temperature of 2.2K between 1979/80 and 2004/5 in channel 1. Thompson *et. al.* (2012) highlighted the discrepancies between both time series. Brindley *et. al.* (1999) (hereafter referred to as BRINDLEY) also include a time series for channel 1 from 1979 until the beginning of 1995. Here, problems in the processing of SSU data and differences in the data availability are noted, especially for LIU, and the tidal corrections are discussed in detail. In response to Thompson *et. al*. (2012) Zou (personal communication) has been reprocessing the NOAA-CLASS archive data set. Results from this reprocessing were presented at the SPARC[3] temperature trends meeting in Reading University, September 2013 where it was agreed that the official SSU level 1b dataset would be that stored at the NOAA-CLASS archive, using the space view count corrections supplied by the Met Office.

In this paper we have used two versions of the level 1b SSU datasets to generate a final model independent analysis. The first “Met Office” time series was based on real time analysis of the SSU data, up until about 1997 and later from NOAA in collaboration with

[3] Stratosphere-troposphere Processes And their Role in Climate

A.J. Miller and R. Lin of the NOAA Climate Prediction Center (personal communications). A second analysis has now been made using the level 1b radiances from the CLASS archive to estimate temperature trends using the Met Office tidal adjustment, Met Office PMC pressure cell compensation, space view counts correction and Met Office technique for matching between spacecraft to generate a final model independent analysis. This analysis is designated as the "NASH" time series.

An important application of the SSU dataset has been the assimilation of the SSU radiances directly in reanalyses (e.g. ERA-40 and ERA-Interim, Uppala *et. al.* 2005). Exploiting the SSU measurements in this way requires a homogenous radiance dataset based on the best knowledge of the calibration and uses all scan angles but doesn't require a tidal correction. There have been some studies on this and also on comparing the consistency of SSU radiances with AMSU-A stratospheric channel radiances using the ERA-40 reanalysis (e.g. Kobayashi *et. al.* 2009).

This paper documents the production of the stratospheric temperature record from the SSU measurements by the Met Office and compares the results with other reprocessed SSU datasets. We report here the adjustments needed to make the measurements as consistent in time as possible and secondly estimate the uncertainty in the time series after these adjustments have been made. The paper is arranged as follows, section 2 describes the SSU instrument and the history of the data processing, section 3 describes the calibration procedure and tests, for users of the level 1b calibrated radiance data. Section 4 describes the determination of the channel spectral characteristics of the SSU and section 5 shows the influence of solar tides on the twice daily measurements. Section 6 presents the temperature time series for inferring trends and section 7 summarises the conclusions.

2. Overview of the SSU instrument and its measurements

2.1 Principles of operation of the SSU

The SSU used the selective chopping technique developed by Houghton and Smith (1970), combined with the pressure modulator technique used in the Pressure Modulator Radiometer on Nimbus-6, Curtis *et. al.* (1974). A schematic of the optics for one channel of the SSU channels is shown in Figure 1. Radiation centred at 665 cm^{-1} was filtered through a Pressure Modulator Cell (PMC) and a supplementary interference filter of bandwidth 60 cm^{-1}. Radiation from spectral regions where pressure modulation of the cell did not result in a transmission modulation through the PMC was rejected. This corresponded to regions of strong absorption close to the carbon dioxide line centres

and regions of negligible absorption in the line wings. The regions of transmission modulation were further away from the line centres in a high pressure PMC than in a low pressure PMC. Channel 1 with a high pressure PMC sensed radiation with a lower

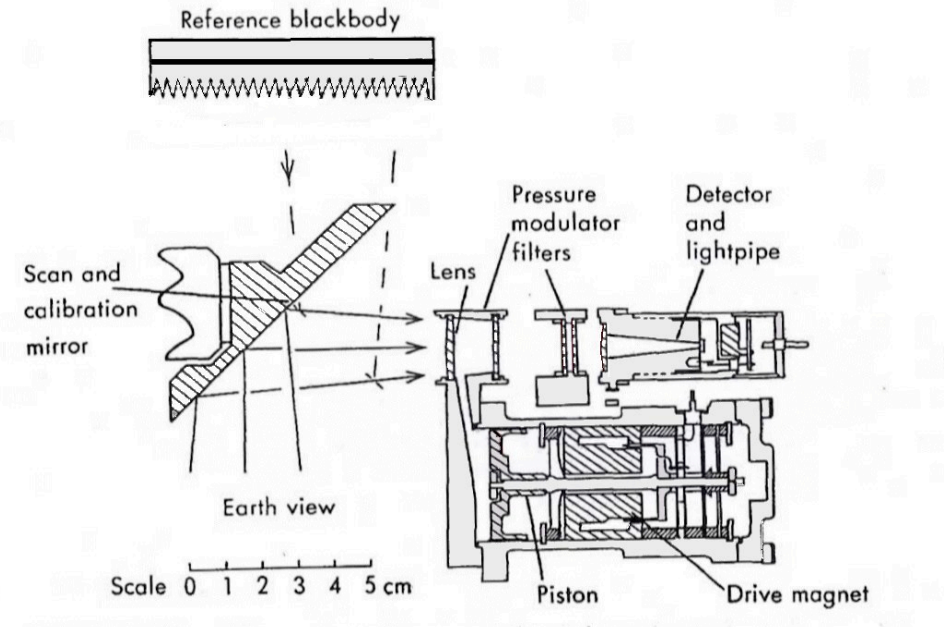

Figure 1. Schematic of the optics and pressure modulator for one cell. All three PMCs used the same mirror. Lens and light pipe windows were coated germanium.

carbon dioxide absorption coefficient overall and hence lower down in the atmosphere than that sensed in channel 3 with a lower pressure PMC. The PMCs were connected to a sealed titanium cylinder, where modulation of the pressure was induced by the oscillation of a closely fitting piston, suspended on two diaphragm springs. This piston was maintained in oscillation at its resonant frequency by pulses of current passed through a coil mounted on the piston's shaft and lying in the gap of a magnet. An electronic servo system, which sensed the back-e.m.f. in the coil, controlled the length of the current pulse and kept the amplitude constant. The current to drive the piston was fed into the coil via a ceramic lead-through, see Figure 1. The frequency of the PMC depended on the PMC pressure and the mechanical constants of the spring (assumed to be constant.) The PMC was operated at a stable temperature, normally close to 30°C. The signal channel electronics amplified and selected the signal component from the detector in phase with the pressure modulation. The three PMCs in the SSU were mounted close to each other, in parallel facing the plane scan mirror.

A plane mirror scanned sideways in 8 steps of 10 degrees up to 35° either side of nadir. Each view lasted 4s, with data integrated for 3.4s. Every 256s, the mirror rotated to observe an internal reference blackbody at a temperature around 295K for 16s and then a space view for 16s. Earth view radiances were derived from a linear interpolation

between the space view radiance and the internal black body radiance. The SSU signal was smallest for the internal blackbody view radiance and largest for the space view radiance. If the output of the signal channel was X_{sc} counts, and the radiance viewed was R_{sc}, then:

$$R_{sc} = -A.X_{sc} + B \quad (1)$$

Where *A*, and *B* were constants over a 4 minute calibration cycle. *A* depended on the detector performance, the electrical amplification, and the amplitude of the pressure modulation, and *B* included the amplitude of the pressure modulation and the electrical offset for cell temperature modulation.

The viewing angles of the SSU were very stable during operation, although different SSUs will have had slightly different angles depending on the stepper motor. In the Met Office time series only the zonal radiances of the near nadir views, positions 4 and 5, were used so that there was no need to compensate for the limb-brightening in the other views. Where off-nadir views have been used, for instance to compute synthesised channels (see later) or the pressure dependence of the SSU observations, these were differences between the average of views 1 and 8 at the edges of the swath from the average of views 4 and 5 although note these are not viewing the same scene. For this to be reliable, daily data coverage from ascending and descending orbits needs to be complete, and anomalous values obtained for limb brightening were a strong indicator of inadequate data coverage.

2.2 History of the SSU data processing

All SSU data processed in the Met Office were from the data received by NOAA in near real time and sent daily in two data streams,

- Earth located level 0 SSU output including the radiometer counts and housekeeping information (i.e. the raw data)
- Earth located calibrated data, which NOAA had converted the counts from selected TOVS instruments including the SSU channels, into radiance values.

The processed data stream from NOAA was used for all daily operational products at the time such as routine stratospheric monitoring by the forecasters. The Met Office processing was described in Pick and Brownscombe (1981) and is summarised in section 3 for completeness.

Data reception at the Met Office from 1978 to 1990 is summarised in Bailey *et al* (1993) and for the rest of the operational time series it has been verified that there was less

than 3 months in 1995 when data were completely missing in the Met Office time series analysis.

Reprocessing from raw data was necessary when satellites lost their operational status as they were replaced by newer satellites. NOAA-9 lost its operational status in March 1987, and after that only the raw NOAA-9 SSU data were transmitted to the Met Office.

After 1998 with the introduction of AMSU-A the SSU observations were no longer available for real time stratospheric monitoring in the Met Office and so they were only collected by NOAA and subsequently included in the Met Office time series in collaboration with the NOAA Climate Prediction Center

The Met Office evaluation of the SSU radiances was based on 5 day averages of radiances from ascending and descending orbits separately, in latitude bands of 10° from 75° N to 75°S. The differences between ascending and descending orbits were checked against the expected values, similarly limb brightening was checked against expected values and the standard deviations of the zonal means were also checked, see Nash and Forrester (1986). If these quality checks were met, showing that data coverage was sufficient for further analysis, the average of the ascending and descending orbits would be combined with other valid 5 day averages to give a 30 day average for use in further evaluation (to avoid complications from variations introduced by lunar tides).

For this report the SSU level 1b radiances from the NOAA-CLASS archive were also obtained and corrected as described here and referred to as the “NASH” time series. The CLASS archive has some data missing in the 1980’s, and some of the basic time series have small differences from what was observed in the Met Office time series so it was decided to retain both analyses here. The real time SSU radiances received at the Met Office were not kept and so the CLASS archive is now the only repository of level 1b data users can access.

2.3 SSU data reprocessing for climate monitoring

The reprocessed SSU data, from which the results presented in this paper are all derived, have had several processing steps applied. The various steps are listed below and described in more detail in the sections indicated.

I. Convert the raw counts to calibrated level 1c radiances which are archived and used for assimilation in reanalyses (section 3.1). Note that in the NOAA-CLASS archive the digitisation of the raw radiances is reduced compared to the original SSU data with the raw counts divided by 4 to give counts in the range 0 to 999. In this paper "counts" refer to the values extracted from the CLASS archive and multiplied by 4 to match the original real time dataset.
II. Zonally average the radiances into latitude bands to derive daily, 5 day, monthly and 120 day means (section 3.2)
III. Derive synthetic channel radiances used as a check on the basic SSU channels (section 3.3)
IV. Develop an accurate forward model for the radiances to derive weighting functions for optimal assimilation in reanalyses and to infer mean layer temperatures for time series analysis (section 4). This includes calculating a spectral response function from the cell pressures and allowing for increasing carbon dioxide concentrations.
V. Merge all the corrected SSU derived layer mean temperatures from each spacecraft using NOAA-6 as the reference by computing the mean differences during overlap periods (section 6). This includes applying an adjustment for the influence of the solar tides (derived by empirical analysis of early SSU data) to calculate accurate daily means (section 5).

In addition to these steps an error budget is computed and validated by comparing the same SSU measurements from different spacecraft. This enables realistic uncertainties to be computed on the final temperature trends.

3. Met Office processing from counts to calibrated radiances

The procedure for the basic calibration of the TOVS radiometers, including the SSU, is outlined in Lauritson *et. al.* (1979) and essentially uses equation 1 to convert counts to radiances with the calibration coefficients included in the raw data. Radiances were converted to equivalent black body brightness temperatures (hereafter referred to as brightness temperatures) using the inverse of Planck's radiation equation. The earth-located brightness temperatures were stored as the level 1b dataset for SSU.

3.1 Prelaunch tests

There was a dedicated effort at the Met Office to confirm the in-orbit calibration through a detailed pre-launch characterisation of the SSU instruments in the laboratory before launch. By early 1978, laboratory testing had identified a problem with the space view observations reported by Pick and Brownscombe (1981). An electrical offset was induced in the signal channel outputs during space view which was not present in the

outputs for the rest of the observing cycle. By inhibiting the scan mirror in the space view, the counts offset would be apparent only when the space view observations were made. During space views, the platinum blackbody temperature sensor switched to a reference mode. The platinum temperature sensor circuit was faulty and oscillated at high frequencies, and so the radio frequency interference within the SSU changed when the circuit switched to the reference resistance. Inhibit tests for the space view were performed in space on TIROS-N, NOAA-6 and NOAA-7, giving space view count corrections similar to those in the laboratory. Table 1 shows the size of the space view count corrections (defined as the true space counts– uncorrected space counts) for all the SSUs. Without this space view correction a bias in SSU scene radiance was observed which varied linearly from a space view radiance to zero at the internal black body radiance. The space view counts of channel 1 of TIROS-N needed to be reduced by 16 counts so without this correction a radiance of about 50 mW m^{-2} sr^{-1} cm^{-1} would have a positive bias of around 0.5 K, and for a similar radiance, NOAA-6 channel 1 , with the space view counts too low by 20 counts would have been too low by about 0.7 K without a correction applied.

	Space view correction in counts		
Spacecraft	Channel 1(25)	Channel 2(26)	Channel 3(27)
TIROS-N*	-16	8	Failed
NOAA-6*	20	9	12
NOAA-7	0	xx	5
NOAA-8	-3	-9	-26
NOAA-9	2	-34	0
NOAA-11	10.5	-2	2.5
NOAA-14	0	-12.5	11

** values taken from Pick and Brownscombe (1981)*

Table 1. Space view correction estimates using the raw level 1b archive to obtain consistent radiances between spacecraft after differences in PMC pressure and tidal differences have been corrected using the Met Office correction scheme. Note that the data in the NOAA CLASS archive has assumed a larger space view correction for NOAA-9, NOAA-11 and NOAA-14 channel 2.

With space view anomaly corrections applied, Pick and Brownscombe (1981) found the average difference between TIROS-N and NOAA-6 channel 1 observations to be 0.12 mW m^{-2} sr^{-1} cm^{-1} (samples between July 1979 and April 1980). This radiance difference is equivalent to 0.12 K in brightness temperature. Apart from TIROS-N and NOAA-6 the original records of the space view corrections have been lost both in the Met Office and at NOAA. Table 1 gives estimates of NOAA-7 to NOAA-14 corrections derived by finding the radiance differences between spacecraft in the NOAA-CLASS archive as contained in the basic NOAA data set as presented by Zou (personal communication) after adjustments for cell pressure and tidal corrections have been applied.

The space view corrections applied by NOAA to the real time observations from the first SSU on TIROS-N were incorrect, and so the Met Office reprocessed all the TIROS-N observations from the raw data stream. For the WANG dataset the equivalent difference in the basic brightness temperatures between the TIROS-N and NOAA-6 channel 1 was 1.3 K. Hence it can be inferred that space view corrections cannot have been applied by WANG in generating their TIROS-N and NOAA-6 radiances. Comparison of the basic radiances in WANG for NOAA-7 and NOAA-9 shows that these were also different to the NOAA real time processing used by the Met Office. BRINDLEY had similar radiance values from the Met Office data set, with only NOAA-9 having significant radiometric anomalies needing special correction for the time series analysis. A NOAA-9 radiance anomaly correction was performed by BRINDLEY. This anomaly is discussed in section 3.2.2, and shows that for NOAA-9 something changed between operation in the laboratory and operation in space. This was the only SSU where this occurred.

The data distributed by NOAA in real time with space view count corrections were not archived permanently by NOAA at the time, but were forwarded to the Met Office and the NOAA Climate Prediction Center and some other users. The NOAA-CLASS archive was generated from level 1b information, without any space view correction being applied. So both the LIU and WANG datasets had SSU radiance errors caused by this omission.

For the calibration stability the SSU internal black body was assumed to have an emissivity of one, with its temperature given by three thermistors mounted close to its surface. The SSU platinum resistance thermometers (PRTs) on the internal black body were not used in the Met Office processing due to concerns about their noise levels and reliability. Hence, the long term stability of the internal black body reference relied on the stability of the thermistors. In space the blackbody surface was shielded from direct sunlight, and so there was no reason to expect the radiation emitted from this view to change during an orbit, unlike the problems seen with the MSU blackbody, Zou and Wang (2010).

Once space view corrections had been applied, the tests at the Met Office demonstrated that the uncertainties in measured radiances were as listed in Table 2. Self-calibration refers to the estimated uncertainty in the blackbody/space views which are used for the calibration applied to the earth scenes. The radiometer is assumed to have a linear response of counts against radiance, so non-linearity refers to the possible radiance errors from this assumption. The uncertainty in space view offset comes from the results

of inhibit testing in the laboratory and in space for the early spacecraft. In orbit short term change refers to the uncertainty induced by short term small scale fluctuations in the observed radiances, e.g. representativeness errors as introduced by small scale gravity waves. The radiometric offset due to water vapour in the PMCs was a theoretical computation, based on the testing performed on PMCs with known water vapour contamination. Most of the SSUs were re-tested at the Met Office shortly before launch to quantify any spectroscopic changes and radiometric tests were also performed.

	Channel 1 [K]	Channel 2 [K]	Channel 3 [K]
Self-calibration	0.1	0.09	0.08
Non-Linearity	0.05	0.042	0.04
Space view offset	0.02	0.026	0.03
In orbit short term change	0.05	0.042	0.11
Radiometric offset due to water vapour in the PMC changing spectral response	0.02	0.04	0.08
Overall radiometric precision	0.13	0.12	0.17
Random error in individual earth observation	0.3	0.4	0.5

Table 2. Error budget of SSU Radiance observations (for averages in space or time) in brightness temperature after Nash and Brownscombe (1982), given a correct space view offset correction.

3.2 Averaging of radiances

In order to analyse the stratospheric temperatures and compare measurements from different spacecraft the individual radiances are averaged together as zonal means in 10 degree latitude bands. This averaging was also performed on the SSU housekeeping information from level 0 data, such as PMC frequencies, SSU temperatures, space view and blackbody counts, calibration coefficients ,etc.

Zonal means were produced for each Earth view scan position so the stability of the limb-brightening could be monitored as 0.5*[(EA1+EA8)-(EA4and EA5)]. The variation of tide with local time of day was estimated from the difference between (EA1-EA8), see Brownscombe *et. al.* (1985). The temperature trends reported here were derived from an average of the nadir views EA4 and EA5. Standard deviations of all the zonal means were computed, as was the difference between ascending and descending orbits. The radiance evaluation was then based on averages over 5 days, where data coverage was sufficient to avoid artefacts in the difference between ascending and descending orbits. In addition, it was required that standard deviations of the zonal means at high latitudes

were compatible with the standard deviations of the zonal means in the tropics. This was because the standard deviations of zonal means would increase rapidly at high latitudes, especially in winter months, if data coverage was poor. Thirty day means were used for the time series, and means over about 120 days (in 10 degree latitude bands) were used for matching observations from different spacecraft during overlap periods.

3.3 In-orbit performance

3.3.1 Radiometric noise

An assessment of the radiometric performance of the SSU instruments in-orbit was based on a comparison of zonally averaged nadir view SSU radiances from two different SSUs in stable orbit at the same time, e.g. between NOAA-7 and NOAA-6 (see Nash and Forrester (1986) for more details of the technique). With two SSU's in simultaneous operation, 120 day zonally averaged radiance comparisons were used for comparison. The standard deviation of the differences between the globally averaged radiances of the two SSU's over 120 day periods was computed and compared with the standard deviation of the differences for daily samples of zonally averaged radiances, as listed in Table 3. The long term standard deviations were higher than would be computed from the daily values given in Table 2 divided by the square root of the number of earth view observations in the 120 day period. Possible causes of this are outlined later in this section.

The technique used for matching successive spacecraft in the time series analysis, was ideally to use an overlap period of at least 120 days. Even when there was little overlap between spacecraft, the average for 120 days at the end of one spacecraft operation was matched with 120 days at the start of the next spacecraft. However, it was preferred if the overlap period used did not include the first 100 days of the new SSU operation, as this allowed time for the new system to settle down and outgassing of some contaminants to occur, before comparisons were started. After this time the 120 day standard deviations in the differences between spacecraft give a good guide as to the uncertainty associated with matching the radiances from the two spacecraft, and so indicate the uncertainty to which data from the two spacecraft can be merged by this technique.

The random errors in the difference between zonally averaged SSU radiances for a 10° latitude band for SSU channels 1 and 3, plus two synthesised channels (see later) were higher than the errors in the global radiance comparisons. The 120 day analysis was much less reliable for channel 2 because the instability in NOAA-7 led to small sample

sizes compared to channels 1 and 3. The HIRS/SSU synthesised channel 35X was included since it peaked at a similar height to channel 2. For the basic channels the random errors in the daily zonal averages were about twice as large as the random errors in the global averages. However, the random errors in the synthesised radiances reduced by about an order of magnitude in the global averages relative to daily zonal averages. Thus, when SSUs were in simultaneous operation, the synthesised channels could be matched to the preceding spacecraft with an uncertainty in global radiances only slightly larger than the basic channels.

Temperature [K]	Latitude band	Channel 1	Channel 2	Channel 3	Channel 35X	Channel 47X
St. dev. for daily averaged spacecraft differences	10° average	0.13	0.12	0.17	0.6	1.2
St. dev. In average spacecraft difference for 120 days	75°S to 75°N	0.074 ±0.01	0.094 ±0.007	0.11 ±0.025	0.11 ±0.05	0.16 ±0.04

Table 3. Standard deviation in the zonal radiance differences from NOAA-7 and NOAA-6 in simultaneous operation for daily averages after Nash and Brownscombe (1983), and Nash (1988), and for the standard deviation associated with 120 day differences between global averages.

Random errors for 10° latitude bands as a function of latitude in the differences between seasonal brightness temperature averages are plotted in Figure 2 for channels 1 and 3 and the synthesised channels 35X and 47X. Errors were mostly higher than the random errors in global averages, apart from between 15°N and 35°N. For the basic channels an overlap of three or four months is sufficient to establish the relative performance of two operational SSUs in terms of global means. However, for individual zonal radiances it is more difficult to establish the relative performance of the spacecraft, particularly at high latitudes, both because of the increased uncertainty and the greater variation in temperature anomaly month to month. Hence uncertainty in time series of individual latitude bands will be higher than in the time series for global means. The increase in random errors for the individual 10° latitude bands relative to the global means occurred for the following reasons:-

- Limitations in spatial and temporal coverage cause larger uncertainty in sampling the planetary waves in the atmosphere at high latitudes. This error is larger for synthesised channels because of the difficulty of measuring the limb brightening to the necessary accuracy when data coverage is less than ideal.
- The effects of spectroscopic errors (see 4.3) vary significantly from month to month at high latitudes e.g. the high random errors in channel 3 at high latitudes.
- Differences from all seasons have been combined, but the semi-diurnal temperature tides vary month to month and between seasons, see section 5.

- Gravity waves with longer vertical wavelengths and high phase speed induce temperature variations in the stratosphere, more easily detected in slant paths than in nadir views. In the summer hemisphere convection in the troposphere produces a relative maximum in temperature variance between 10°S and 30°S throughout the stratosphere and lower mesosphere, see Wu and Waters (1996) and Alexander and Barnett (2007). Gravity waves will increase uncertainty in limb-brightening measurements used to generate synthesised channels rather than in nadir views of the basic channels.

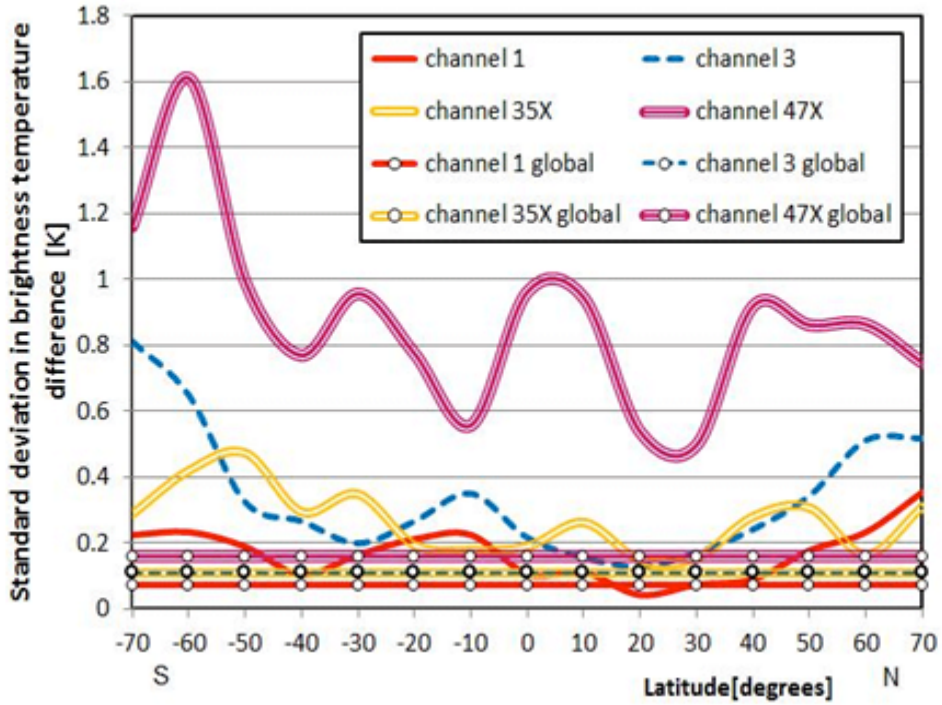

Figure 2. Variation with latitude of the standard deviation of the difference between observations by different spacecraft in simultaneous operation for seasonal zonal averages for SSU channel 1 and channel 3 and synthesised channels 35 X (observing near SSU channel 2), and 47X centred in the lower mesosphere at about 52 km. The random error found in differences between radiance averaged from 75°S to 75°N are included for comparison, as straight lines with values less than 0.2 K.

3.3.2 Systematic biases observed between spacecraft

TIROS-N, NOAA-7 and NOAA-9 all observed with orbit crossing times at the equator near 15:00Z local time, and NOAA-6 and NOAA-8 observed at the equator close to 19:30Z. The mean differences between an SSU observing at these different times depended on:

- The radiometric bias of the two SSUs
- Spectroscopic differences between the two SSUs, (see section 4)
- Differences from bias in the migrating solar temperature tides, (see section 5)

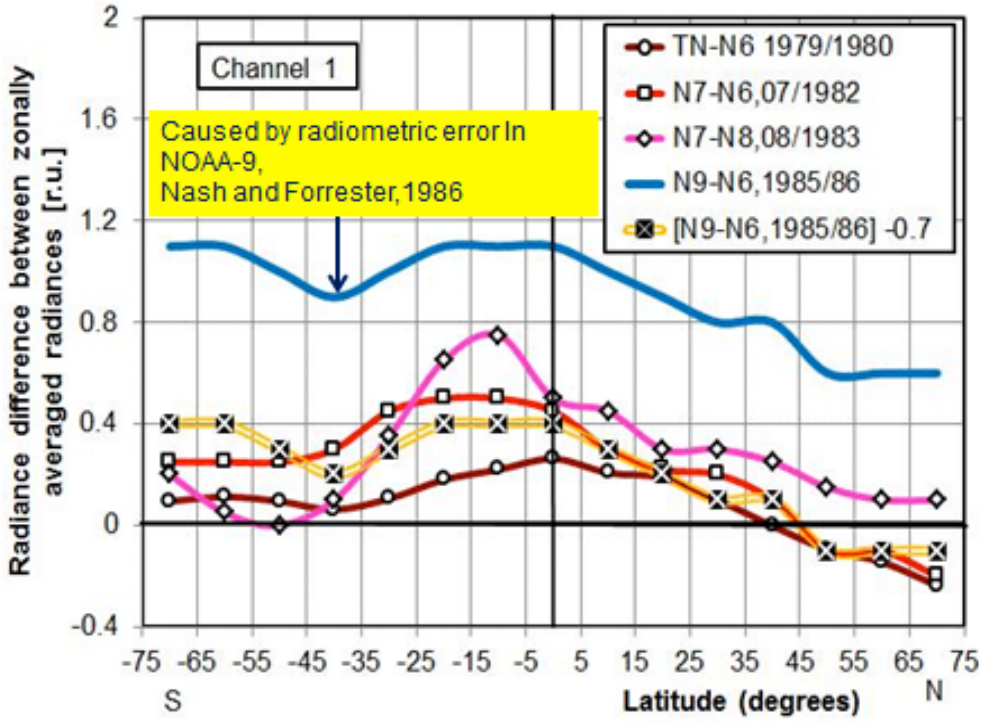

Figure 3(a) Comparison of SSU channel 1 global mean radiance observations between NOAA spacecraft in simultaneous operation, including values from Pick and Brownscombe (1981), with one observing near 15:00 and the other near 19:30 local time.

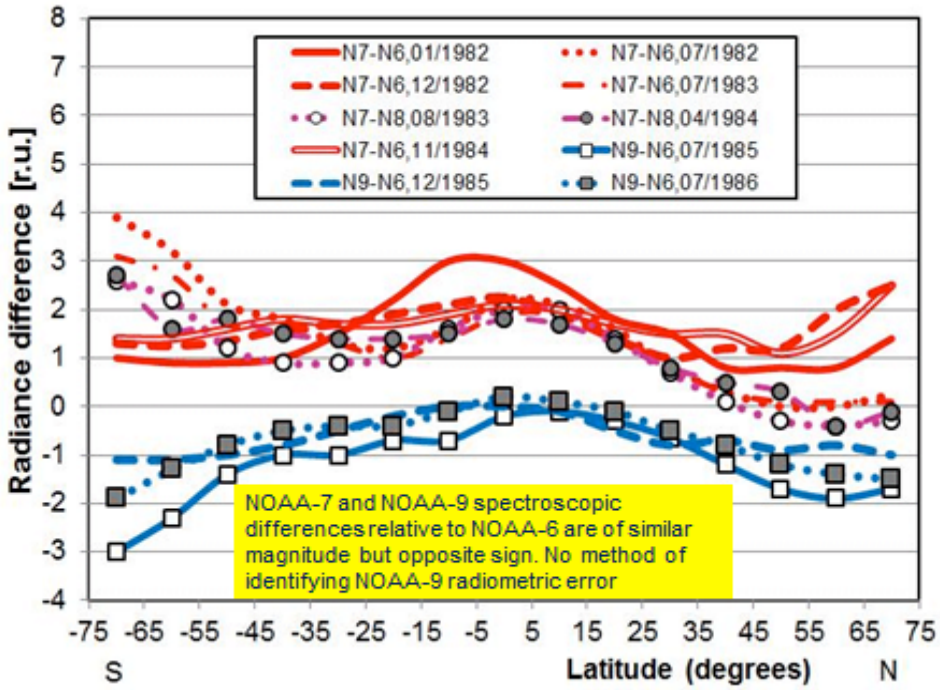

Figure 3(b) Comparison of SSU channel 3 global mean radiance observations between NOAA-spacecraft in simultaneous operation, with one observing near 15:00 and the other near 19:30 local time.

Figure 3(a) and Figure 3(b) show seasonal comparisons (at least 1 month's data in each comparison) for channels 1 and 3 respectively on early NOAA spacecraft. Apart from the

TIROS-N data, all the other data in Figure 3 were from real time NOAA processed observations, with no additional processing by the Met Office. If NOAA-9 channel 1 radiances were reduced by a constant offset of 0.7 mW m^{-2} sr^{-1} cm^{-1}, [0.7K in brightness temperature] the differences with NOAA-6 would be similar to the other spacecraft differences for channel 1 see Figure 3(a). Nash and Forrester (1986) identified that NOAA-9 channel 2 also needed to be reduced by 0.4 K to be consistent with earlier spacecraft. The reason for this was the space view anomaly corrections were incorrect for NOAA-9 in the Met Office real time processing. It is likely that for some reason the space view offset changed between laboratory testing and in space operation. In the laboratory the NOAA-9 observations were within the uncertainty indicated in Table 2.

The NOAA-9 observations could be reprocessed with revised space view corrections to remove the anomaly in an updated dataset, but this has not been done in any data forwarded by the Met Office, e.g. the data sent to BRINDLEY. The differences for channel 3 in Figure 3(b) show NOAA-6 and NOAA-8 were close in performance, but NOAA-7 and NOAA-9 were further apart, mostly the result of spectroscopic differences (see Figures 7 and 8). At high latitudes the winter time differences between NOAA-9 and NOAA-6 were quite different from summer time as the spectroscopic differences at these latitudes were not stable with time of year, see Figure 8, due to changes in the atmospheric state. The failure to use space view corrections in the processing of WANG produced large biases between the early SSUs, especially in channel 1, which are not present in the other SSU time series analyses.

3.4 Synthesised radiances

Five synthesised channels can be computed from the basic SSU channels using the limb-brightening of the TOVS radiances to extrapolate in the vertical from a basic SSU channel, see Nash (1988) for details. These channels can be used as an independent check on the basic channels. For example using HIRS-2 channel 2, a similar weighting function to that of the SSU channel 1 can be obtained. The radiometric properties of these “channels” are shown in Table 4, along with the computed uncertainty. These synthesised channels provide radiances with improved vertical resolution at more or less the same height as the 3 basic channels. Retaining the same channel numbering as in Nash (1988) we have:-

- 35X computed from HIRS-2 channel 2 and the limb-brightening of SSU channel 1 providing a radiance at a similar height to SSU channel 2. These data were included in Ramaswamy *et. al.* (2001). The formula used for the channel was similar to that

used for channel 36X in Nash (1988), with channel *k* defined as HIRS-2 channel 2, and the limb-brightening in channel j is from SSU channel 1 in this case

- 26X providing a radiance from SSU channel 3 and the limb brightening of SSU channel 2 at a similar height to SSU channel 1
- 36X providing a radiance from SSU channel 1 and the limb brightening of SSU channel 2, at a height similar to channel 3
- 47X providing a radiance from SSU channel 2 and the limb-brightening of channel 3 in the lower mesosphere, but the weighting function of this channel differs between the tropics and high latitudes, see Figure 6.
- 15X providing a radiance from SSU channel 2 and the limb-brightening of SSU channel 1, peaking at a height between MSU channel 4 and SSU channel 1.

The changes in global brightness temperatures from these synthesised channels are similar to the associated basic channel, as shown later and support the evidence in the vertical structure of temperature change seen in the basic channels e.g. 26X demonstrates that the spectroscopic corrections applied to channel 3 are reasonable, and that the limb-brightening of channel 2 is consistent with the differences between channel 1 and channel 3 in the basic channels. Where channel 2 does have a break in reliable observations in 1984, 35X provides supporting evidence for the overall channel 2 time series of temperature change from 1978 to 1998, as shown in Figure 16. Channel 15X provides radiances centred at a level between MSU channel 4 and channel 1, and the values shown here include the effects of high cloud in the tropics.

Channel 47X is centred at about 0.5 hPa, but use of the data must take into account the variation of its weighting functions with latitude, see section 4. The improved vertical resolution of the synthesised channels offers a potential advantage when studying features such as the Quasibiennial Oscillation (QBO), where the basic channels only partially resolve the variation of the QBO temperature fluctuations in the vertical. Samples of simultaneous synthesised radiance observations for channels 35X and 47X are shown in Figure 4(a) and (b). The differences between spacecraft for channel 35X are typical of most of the synthesised channels, so radiometric differences between different spacecraft of 1 to 3 mW m^{-2} sr^{-1} cm^{-1} are normal. These do not come from differences in the HIRS-2 channels, but are mostly the result of differences between spacecraft in the limb-brightening observations, where a 3K difference in the synthesised radiance corresponds approximately to a difference of just less than 0.2K in the limb-brightening measurement between spacecraft, with NOAA-9 values higher than NOAA-6 and NOAA-7. 47X has very large differences between spacecraft and this was because

of the large spectroscopic differences between the respective channel 3 observations. The limb brightening of channel 3 was extremely sensitive to the pressure of the PMC, NOAA-7 had the lowest cell pressure and the limb brightening in NOAA-7 was often of the opposite sign to that in NOAA-9 and NOAA-6. Estimates of the tidal contributions to the differences between spacecraft in Figure 4 can be seen in Figure 14.

Components of error budget	**Channel 15X [K]**	**Channel 26X [K]**	**Channel 35X[K]**	**Channel 36X [K]**	**Channel 47X [K]**
Height of weighting fn centre in tropics [km]	22km	28km	36 km	43km	50km
Basic channel	2	3	HIRS2/2	1	2
Limb-br. temp difference from SSU channel	1	2	1	2	3
Standard deviation of synthesised daily zonal radiance, 10° latitude band	0.8	0.7	0.6	0.7	1.2
Error from fov offset 0.1 $mW.m^{-2}$ sr^{-1} cm^{-1} in limb-brightening measurement	2.3	2	1.9	1.9	1.7
Radiance difference caused by a difference in view angles of 0.5°	1.1	1	1.1	0.9	0.7
Total uncertainty in synthesised channel measurements [K]	2.7	2.4	2.3	2.2	2.2

Table 4. Uncertainty of SSU synthesised radiance observations after Nash (1988), but converted to equivalent brightness temperature K. These estimates assume the space view offset correction is applied correctly.

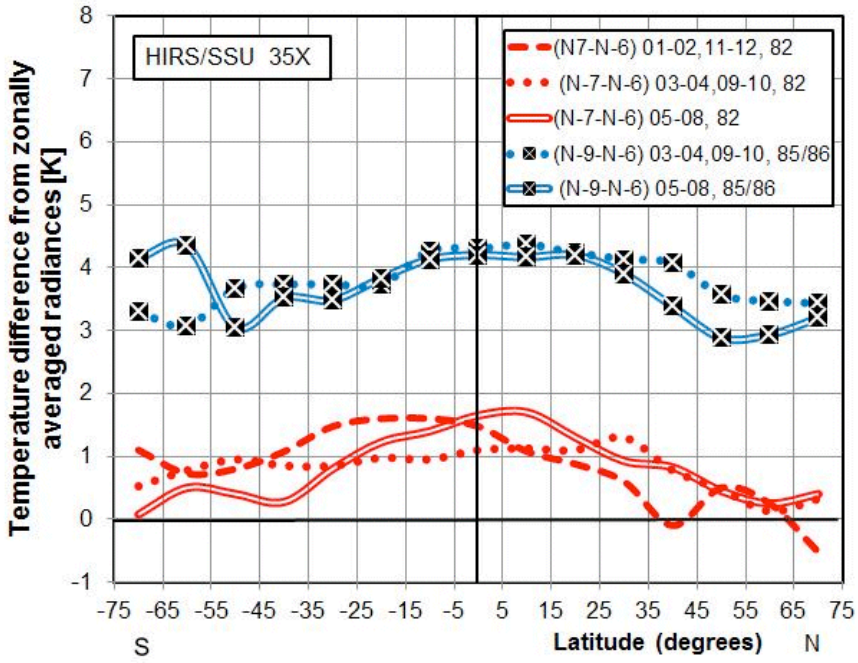

Figure4(a) Comparison of HIRS/SSU channel 35X global radiance observations between NOAA-spacecraft in simultaneous operation , with one observing near 15:00 and the other near 19:30

local time. Samples from November to February, from March, April, September, October, and from May to August

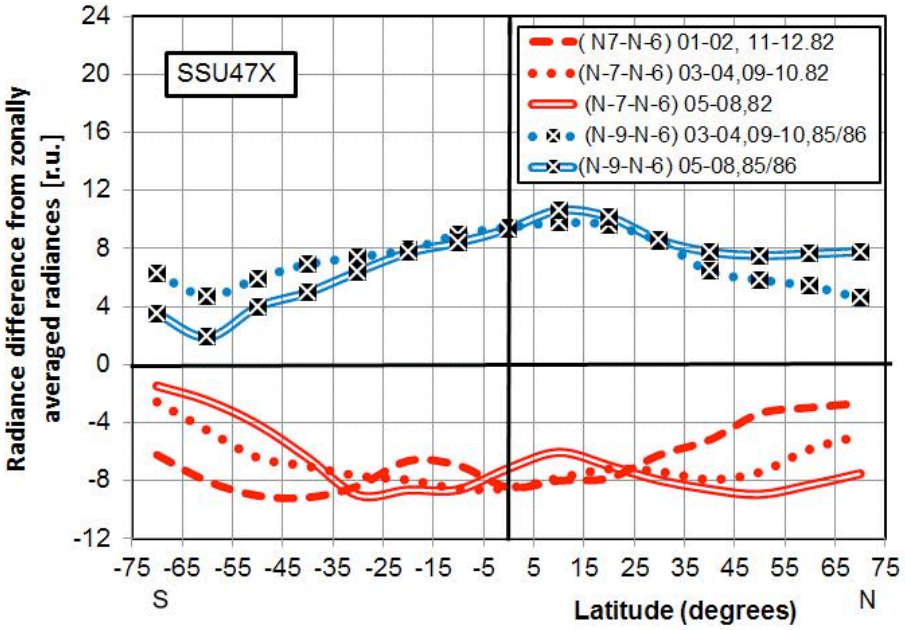

Figure 4(b) Comparison of SSU channel 47X global radiance observations between NOAA spacecraft in simultaneous operation, with one observing near 15:00 and the other near 19:30 local time.

There were two main sources of bias in radiometric comparisons between synthesised radiances on different spacecraft:

(a) Errors in the radiometric quality of the SSU limb-brightening observation. An uncertainty of about 0.1 mW m^{-2} sr^{-1} cm^{-1} in limb-brightening leads to the uncertainty in radiance shown in Table 4. On limited occasions, the bias in limb-brightening error has changed during operation leading to a step change in the global averages of the synthesised radiance. For example a step change of 0.5K in June 1981 in NOAA-6 channel 15X (Nash and Edge; 1989) caused by a change in the limb-brightening of channel 1 of 0.022 mW m^{-2} sr^{-1} cm^{-1}, probably due to a change in the optical path of this PMC, as only one channel was affected. As the synthesised channels do provide reasonable estimates of long term temperature changes with time, see Figures 15 and 17, this indicates that the radiometric stability between different SSU fields of view during a scan cycle is normally extremely high in zonal averages, of the order of 0.01 mW m^{-2} sr^{-1} cm^{-1} or better.

(b) Variation in the angle of view from nadir in the atmosphere for positions 1 and 8. This could be because the average spacecraft orbital height changed with time (see Wentz and Schabel; 1998). NOAA-6 was at an average orbital height of 820 km and NOAA-7 at 855 km. In the years near the maximum of the sunspot cycle the orbital heights of a given spacecraft fell by about 8 km in total over 4 years, and so a small

compensation for the change in height will be required. For channel 15X, each drop in height of about 8 km requires a correction in global means of about -0.025K in brightness temperature. Differences in the view angles can also be significant due to differences in stepper motor settings, particularly if a different type of stepper motor was used for the earth view scan (e.g. the stepper motor on NOAA-9 was a different type to the other SSUs).

Temperature [K]	**Latitude band**	**Channel 15X(rev)**	**Channel 26X**	**Channel 35X**	**Channel 36X**	**Channel 47X**
Standard deviation for daily average spacecraft differences	10° daily average	0.8	0.7	0.6	0.7	1.2
Standard deviation in average spacecraft difference for 4 months	75°S to 75°N	0.15 ±0.03	0.13 ±0.02	0.09 ±0.02	0.10 ±0.03	0.14 ±0.02

Table 5. Standard deviation in the differences from two spacecraft in simultaneous operation for the daily average after Nash (1988), and the random error associated with 4 month differences between global averages from two different spacecraft in simultaneous observation.

When comparing global averages from the synthesised channels, the systematic biases can be removed and the resultant uncertainties then become the values shown in Table 5, just a little larger than the equivalent uncertainty in the equivalent global averages of the basic channels. Synthesised radiances were not computed for channel 35X after 1998, because HIRS-2 channel 2 radiance data were not readily available from the US at the time of the completion of the SSU time series.

4. Spectroscopic performance of SSU

To effectively forward model the SSU radiances the instrument spectral response functions must be known. For SSU this is particularly challenging as it can change in orbit as the cell leaks water vapour and carbon dioxide, which define the cell spectral response and so the response as a function of cell pressure has to be modelled. There was an extensive programme at the Met Office to measure the spectral response before launch to better understand the variations that would be obtained in-orbit. Recent work undertaken for the fast radiative transfer model, RTTOV, (Saunders *et. al.;* 2013) attempts to model the change in spectral response for each of the SSU channels with cell pressure.

4.1. Laboratory testing

During storage in air, immediately after initial construction, most PMCs (apart from the development cells) increased in frequency at an equivalent rate of pressure between 1

to 2hPa per year. Exceptions were the channel 3 PMCs on TIROS-N and NOAA-7. In addition a channel 2 replacement PMC in the early 1980s version of the development model also had leak rates larger than 3hPa per year. When an SSU was stored in dry nitrogen, the rate of increase in frequency was about half that when it was in the moist atmosphere mounted on the spacecraft or in the laboratory.

PMC leaks may have occurred at the crimp on the filling tube, the joint of the filling tube to the titanium body and the electrical lead-through feeding the current for the magnet drive into the PMC, see Figure 1. The areas under suspicion were all coated with epoxy resin to improve the seals, but in the long term the epoxy resin coating was permeable to water vapour. When gas in the PMC was pure carbon dioxide the PMC pressure increased according to the Perfect Gas Law as the PMC warmed to its thermostat temperature. However, once the pressure had increased during storage in the atmosphere, the PMC frequency increased much more rapidly during warm up with water vapour outgassed. 6hPa of water vapour out of a total leak of about 10hPa was found in the PMC when it was tested in the laboratory using a White cell.

Filters, opaque to the far infrared, were superimposed in front of the PMCs and it was found there was no discernible difference between the measurements of transmission through the White cell, whether the filter was present or not, and hence it was concluded that the radiometric effects from water vapour were small (<0.1K) as defined in Table 2.

Transmission through a 10m White cell was measured as the pressure (carbon dioxide nitrogen mix) was reduced logarithmically with time. Tests were made immediately after construction and then later to check the effects of the PMC changes. Spectroscopic computations for the SSU were performed from spectral line data using the instrument parameters and a line by line radiative transfer model assuming a Voigt line shape. The launch pressure advised to users for each PMC was the pressure of carbon dioxide in the PMC that matched the transmission measurements in the laboratory, see Pick and Brownscombe (1981) for more details. The laboratory spectroscopic testing for channels 2 and 3 is summarised in Figure 5, each point on the graph indicating the difference between the initial tests and a test after significant leakage had occurred. This shows that the effective change in PMC pressure for the leak during storage was less than half that expected if the pressure change had been caused by just carbon dioxide leaking. Having identified this problem, the SSU storage environment was changed and instruments were normally stored under vacuum for as long as possible on the ground,

starting with the NOAA-7 instrument. The later SSUs were stored for many years before launch but did not have as large leaks as some of the early instruments.

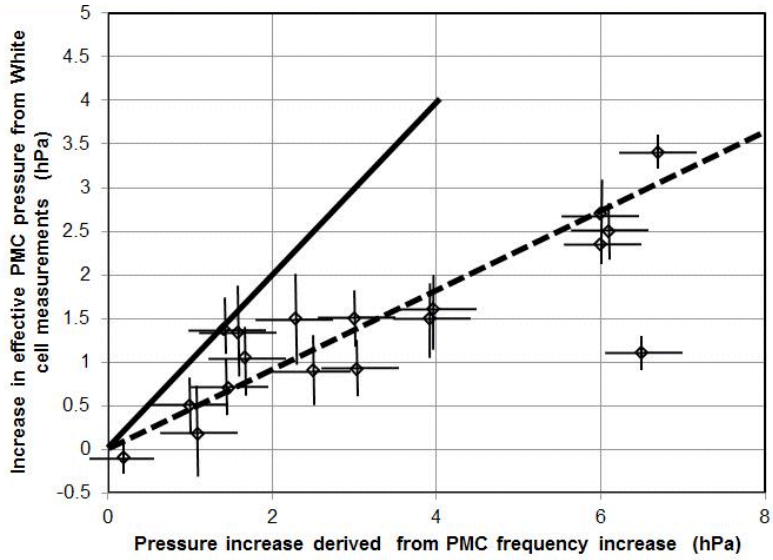

Figure 5. Summary of laboratory spectroscopic testing for channels 2 and 3 in terms of the effective increase in pressure in PMCs from the White cell measurements compared with the pressure increase inferred from the increase in PMC frequency between tests separated by a year or more. The solid line is for an increase in carbon dioxide pressure. The dashed line is 0.45 of the pure carbon dioxide increase, representing the effect of water vapour in the PMC leaks.

4.2 Sensitivity of temperature weighting functions to temperature profile

Basic weighting functions for this paper shown in Figure 6 were supplied by Shine *et al* (2008), (normalised so that $\sum[W*dln(p)]=1$, where W is the weighting function $d\tau/dln(p)$ with τ the layer transmittance and p is the pressure). The concentration of carbon dioxide used in the computation was 350 ppmv which was the value for 1988. The infrared radiances observed by the SSU were not a linear function of atmospheric temperature. A temperature change of 1K at a scene temperature of 265K produced a change in radiance 76% larger than a change of 1K at a temperature of 205 K. This means that the weighting of temperature in the SSU observation will depend on the temperature profile under observation, with significant differences between tropical and polar latitudes. In the examples of typical weighting functions shown in Figure 6, temperature profiles from the CIRA-86 climatology have been selected. Each layer of the basic weighting functions, *W,* was then multiplied by the change in radiance for a change in temperature of 1K, and the result then renormalized. This then showed the difference the temperature structure made to the SSU radiance sampling with the structures shown as TEMP weighting functions in Figure 6. There is also some sensitivity to the ozone profile which is reported by Shine *et. al.* (2008). At high latitudes the temperature profiles are different between summer and winter and examples of the variation of the TEMP

weighting functions for these extremes of the temperature cycle are shown in Figure 6(b), (d) and (e).

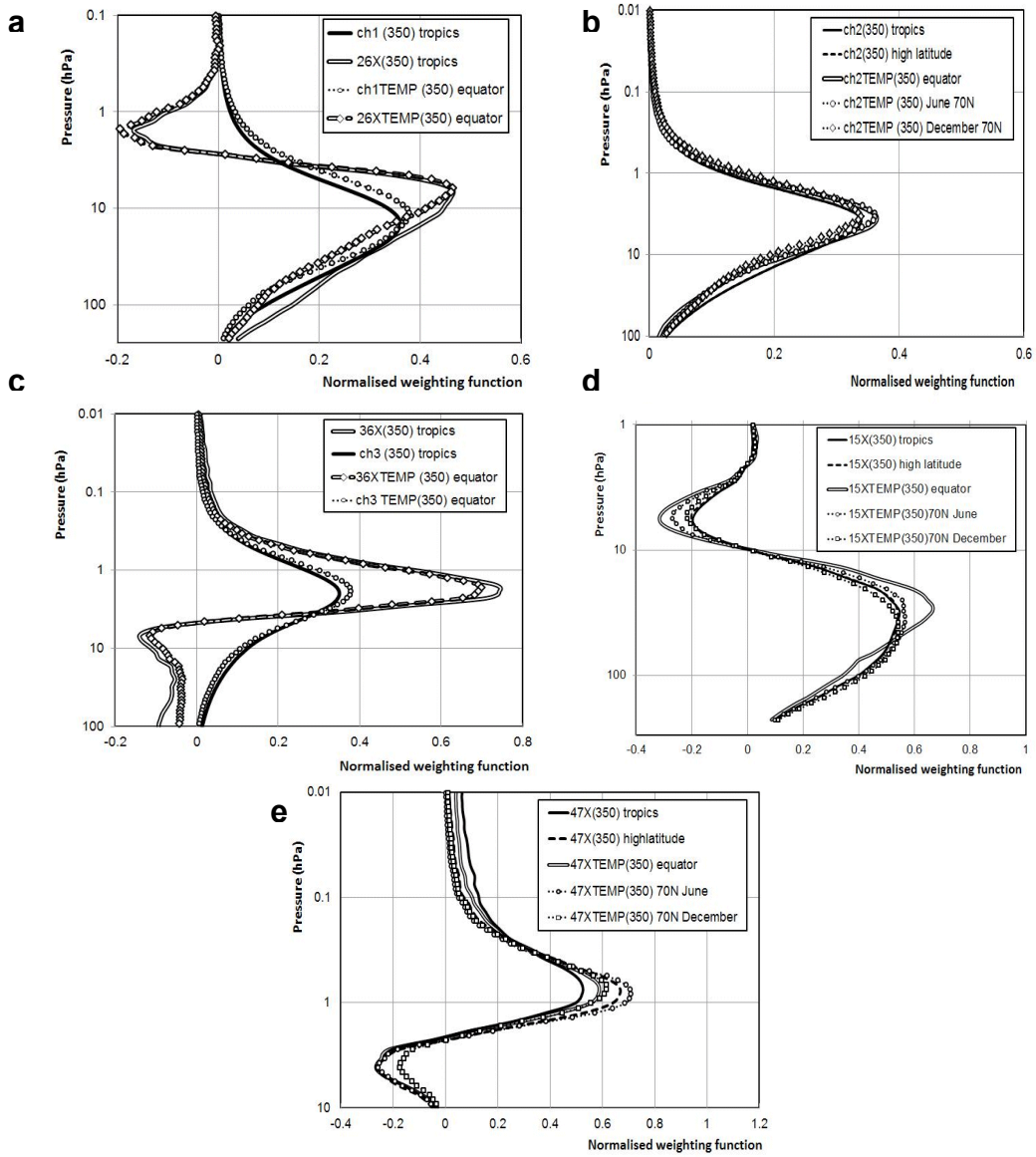

Figure 6. Weighting functions assuming a CO_2 concentration of 350ppmv. (a) channels 1 and 26X, with temperature weighting functions for the equator. (b) channel 2 plotted as (a) for the equator plus June/December at 70° N. (c) channels 3 and 36X plotted as (a). (d) channel 15X plotted as (b). (e) channel 47X plotted as (b).

The atmospheric temperature is coldest at around 100 hPa then increases with height. The non-linearity of the radiances with temperature has the effect of reducing the contributions from cold layers in the profile, increasing the relative contribution at pressures lower than 10 hPa and shifting the temperature layer averages upwards relative to the basic weighting functions. In Figure 6(b) the differences between basic weighting functions for channel 2 in the tropics and at high latitudes are too small to be seen, but once the non-linearity of the infrared radiances is taken into account, the averaging of the temperatures was shifted upwards by a similar amount in the summer

at high latitudes and near the equator, and was shifted further upwards in the winter at high latitudes. In Figure 6(c) the centre of the layer temperature averages for channel 3 and 36X did not shift upwards because these basic weighting functions peak near the highest temperatures. However, the temperature averages had better vertical resolution than the basic weighting functions.

4.3 Spectroscopic assessment after launch

PMC cell pressure changes during the SSU time series are shown in Figure 7. If there was no additional damage to the PMCs on launch, water vapour would leak out quickly in space, but any leak of dry air or carbon dioxide would be less than 10 per cent of the leak rate observed on the ground, Thus, for most PMCs, there should have been little outward leak of carbon dioxide or dry air. There were a few PMCs that effectively had no significant frequency change after launch, especially those on NOAA-6. More commonly, there was a relatively high rate of PMC frequency change with time immediately after launch, reducing exponentially with time to an insignificant decrease after two years in space. This was taken as the characteristic of water vapour leaking from the PMC in space. In the most extreme leak during storage before launch, NOAA-7 channel 3 PMC had a water vapour ingress into the PMC of more than 6 hPa in a leak of 11 hPa at one time, but was reduced by a period of storage in vacuum before launch. On launch this PMC frequency dropped very rapidly with time, with pressure falling by 3hPa but within six months became essentially stable in pressure.

The leak in NOAA-7 channel 2 was larger than the other PMC leaks in space and bore no relationship to the rate of leakage in this PMC during storage before launch. The rate of pressure loss reduced with time to some extent, from 3.9 hPa in 6 months shortly after launch to about 2.5 hPa in 6 months in the second half of 1982, but never became negligible as in all the other PMCs. All the water vapour had probably left this PMC by the beginning of 1983. In total, leakage for this PMC from launch until mid-1983 was probably around 5.5hPa of carbon dioxide, 0.5hPa of dry air and 4hPa of water vapour.

The uncertainty as to the composition of this leak dictated that the correction procedures used for the pressure changes in other PMCs could not be used in this case. Calibration constants for this channel changed very rapidly, especially the offset *B*, in equation 1. As a consequence the internal black body view radiance went out of limits in July 1983, and NOAA-7 channel 2 radiance measurements after this date are invalid. Obtaining accurate corrections for the early part of the leak is difficult, given the uncertainty as to the precise composition of the leak.

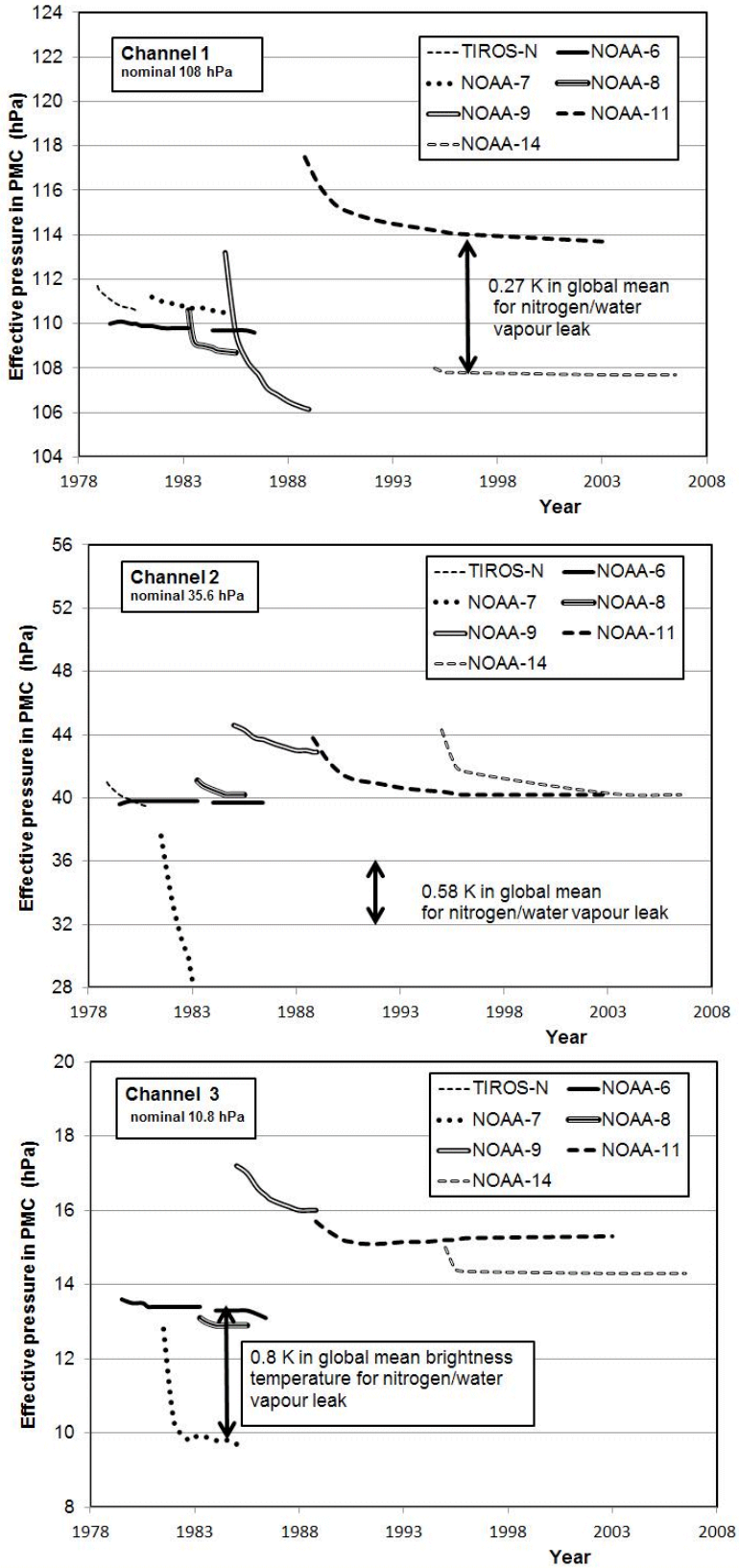

Figure 7. Changes in PMC cell pressures derived from changes in PMC frequencies during operation in space. Effect on global radiances for a typical pressure change is shown, for a typical water vapour PMC leak.

The sensitivity of SSU radiances to water vapour leaks, see Figure 8, was computed from the limb-brightening of the SSU measurements. The magnitude of limb-brightening depends on the vertical temperature structure across the SSU weighting function, and a slant path length in the atmosphere. Thus the equivalent pressure change associated with the shift of the weighting function caused by limb brightening can be calculated. Hence, dividing the limb-brightening brightness temperature change by this equivalent pressure change of CO_2 and then multiplying by 0.45 (based on the results from Figure 5) should give the sensitivity to PMC pressure change in space for a water vapour leak. The limb-brightening of channels 1 and 2 was of similar magnitude in the tropics and mid-latitudes, at about 2 $mW.m^{-2}.sr^{-1}.cm^{-1}$, see Brownscombe *et. al.* (1985) for a typical example of limb-brightening in channel 2, and Nash and Brownscombe (1983) for estimates of sensitivity to a leak of carbon dioxide. Sensitivity to PMC pressure change was found to be relatively uniform with latitude for most of the year for channels 1 and 2.

This empirical method of estimating the correction for cell pressure change in flight was used because the limb-brightening observed by the SSU was not reproduced by the historical data set of rocketsonde temperatures, especially at high latitude. Rocketsondes at the time were the main source of information on temperature structure in the upper stratosphere, lower mesosphere.

The estimates of dependence on PMC cell pressure change shown in Figure 8 correspond closely to the values found by WANG using the CRTM radiative transfer model, Chen *et. al.* (2008), for channel 3. The values found by WANG for channels 1 and 2 were about twice as large as those in the Met Office estimates shown here. These differences are significant and for example for channel 2 affect the magnitude of the cell pressure correction applied to NOAAs 11 and 14, with the higher correction leading to a more pronounced drop in brightness temperature compared to the Met Office time series.

4.4 Correction for increasing concentration of atmospheric carbon dioxide

The increase in carbon dioxide concentration during the period the SSUs were measuring affects the weighting functions and hence the levels at which the SSU mean layer temperatures represent. This affects the stratospheric temperature record. The differences for the increased carbon dioxide concentration of 370 ppmv at the end of the time series were small compared to the values for 350 ppmv, but sufficient to produce changes in the weighting functions which need to be compensated, see Shine *et. al.* (2008). As the increase of atmospheric carbon dioxide through this period was essentially linear from year to year, the corrections for increase applied were linear with time.

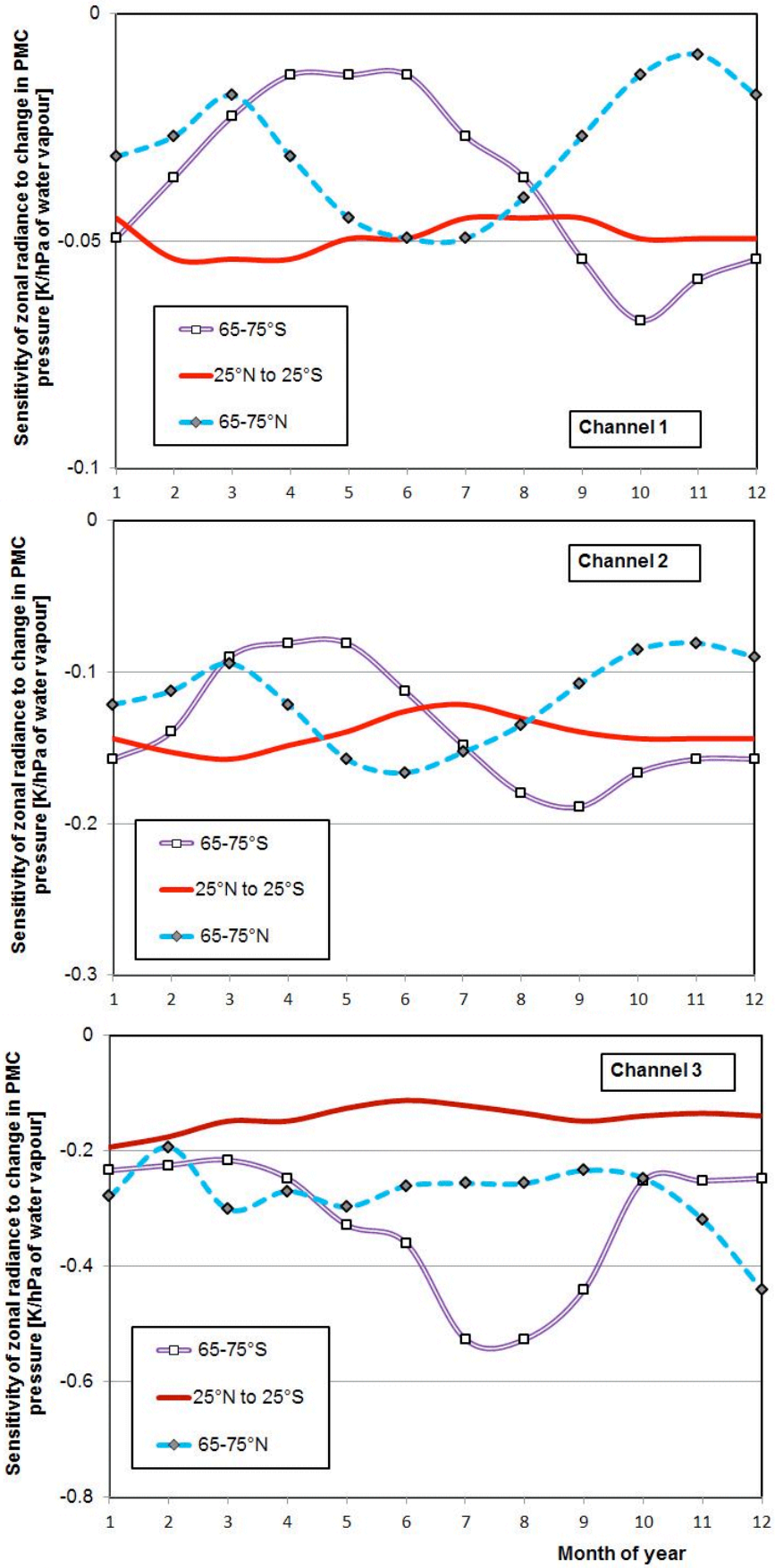

Figure 8. Sensitivity of zonally averaged radiance to a PMC pressure change , (for a water vapour leak) derived from the limb-brightening of the SSU channels, similar to Nash and Brownscombe (1983), for three latitude bands, 25°N to 25°S, 75°N to 55°N and 75°S to 55°S.

The seasonal fluctuation of carbon dioxide each year was not taken into account as this study was concentrating on the year to year changes in brightness temperature. The corrections, relative to 1979, applied here for the increase in carbon dioxide in the atmosphere, through the period of SSU observations (1979-2005) for the basic SSU channels were for 2006 -0.73K, -0.7K and -0.37K respectively for Channels 1 to 3. Corrections used by Wang *et. al.* (2012) were slightly smaller than this at -0.6K, -0.6K and -0.2K for channels 1 to 3 respectively, so this correction only caused a minor difference between the two time series.

5. The influence of solar tides on the SSU time series

5.1 Observations of migrating solar temperature tides

The amplitude of the diurnal tides observed by the SSU was at least as large as the temperature changes seen in the time series analysis. Thus, it is essential that complete ascending and descending orbit information is combined together in a time series analysis to avoid biases due to diurnal tides in the monthly averages.

Solar temperature tidal effects on the SSU radiances at equinox were validated against tidal models in Brownscombe *et. al.* (1985). NOAA-6 and NOAA-7 provided a zonal radiance from each SSU (only using nadir views 4 and 5 combined), with ascending and descending orbit times used separately. Local times of observation for each spacecraft were separated by around 12 hours from 50°N to 50°S, but were closer together at latitudes of 60 to 70°N and further apart at latitudes of 60 to 70°S. The SSU views at 35° from nadir provided additional radiance offsets of at least 20 minutes in local time either side of the nadir views. The amplitudes of diurnal, semidiurnal, terdiurnal and quaterdiurnal tides seen in the SSU observations are shown in Figure 9, with the corresponding phase of the tides in Table 6. Uncertainty in the amplitude was 0.03 K for diurnal and semidiurnal tides, and about 0.05 K for the terdiurnal and quaterdiurnal tides once the results from the 3 channels were averaged together.

Tide	Channel	45-55°S	25-35°S	5°S -5°N	25-35°N	45-55°N
diurnal	3	18:00	17:36	19:00	17:18	17:18
	2	17:42	17:18	17:00	16:48	17:30
	1	17:00	17:18	19:00	17:18	18:00
semidiurnal	3	13:00	12:00	13:12	13:36	10:00
	2	10:30	12:00	13:00	14:00	13:30
	1	11:30	12:00	12:48	13:30	13:30
terdiurnal	1,2,3	13:00	14:00	10:00	11:00	11:00
quaterdiurnal	1,2,3	14:00	14:00	15:00	16:00	16:00

Table 6. Local time of maximum in solar tides, for the amplitudes shown In Figure 9.

The variation with latitude of the diurnal tide in Figure 9(a) is compared with the Hough function (eigenfunctions of Laplace's tidal equation) for the (1,-2) mode for channel 1

and a combination of (1,-2) with a different amplitude and the vertically propagating (1,1) mode for channel 3. This propagating tide has a vertical wavelength of about 28 km, so SSU channel 3 cannot fully resolve the full amplitude of the wave. The phase of this diurnal propagating tide was not adequately modelled in Brownscombe *et. al.* (1985). At the equinox ascending-descending orbit differences are symmetric about the equator, as can be seen for channel 3 in Figure 10. However the amplitude of the diurnal tide in mid-latitudes increases to 1.3K in the summer hemisphere, and in the winter hemisphere reduces to as low as 0.8K. In this case, the tides for modes (1,-2) and of (1,1) were of similar magnitude as at the equinox, but asymmetric diurnal modes for (1,-1) were of amplitude about 0.4 K, and for (1,2) of about 0.2K. The asymmetric modes cause the minimum in the tropics to be displaced away from the equator towards the winter hemisphere.

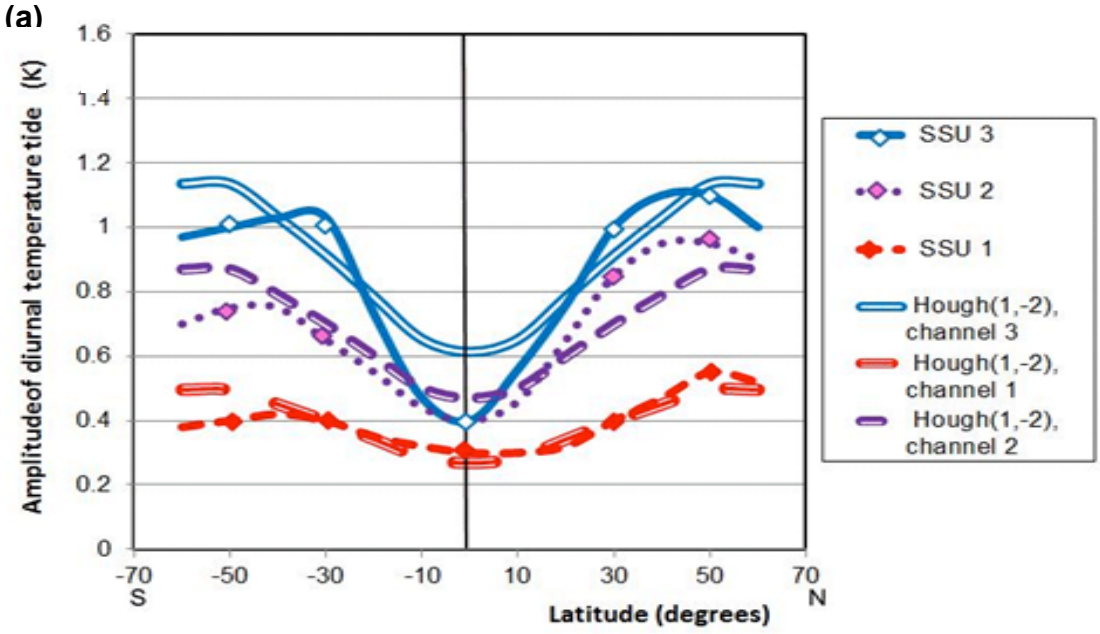

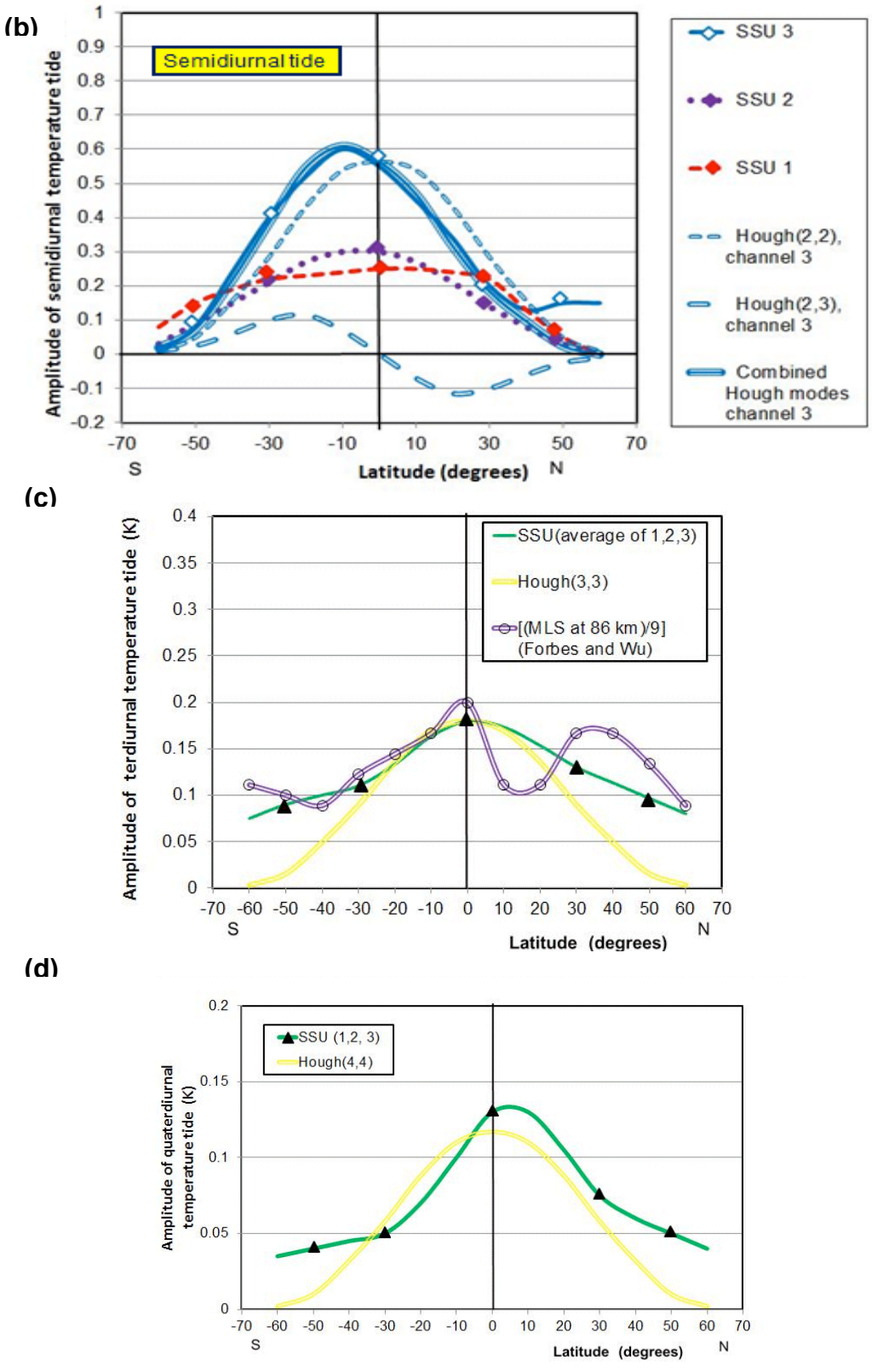

Figure 9. The amplitude of temperature tides in SSU observations, using tidal analysis in Brownscombe et al (1985), for (a) diurnal tide, (b) semidiurnal tide, (c) terdiurnal tide and (d) quaterdiurnal tide.

The values of the diurnal tide for channel 1 in Figure 9 were compatible with the diurnal results for the 1990's from mid-latitude radiosondes in Europe in Seidel *et. al.* (2005) with an amplitude of about 0.5 K at 10 hPa. The diurnal tide in the lower mesosphere, as sensed by channel 47X has a significantly lower amplitude than the tides in channels 3 and 36X.

In contrast, the semidiurnal tides increase in amplitude with height, and values for the amplitude of the semidiurnal migrating tide at 86 km (Forbes and Wu; 2006) were about 8 times as large as those observed by SSU channel 3, but with similar variation with latitude apart from at the poles. For the semidiurnal tide, much of the variation with latitude seen in Figure 9(b) is associated with the (2,2) and (2,3) Hough modes, but the phasing of (2,3) is different to that of the (2,2) mode. Semidiurnal tides dominate the correction required for satellite orbit drift and documentation of these tides in the stratosphere and lower mesosphere is very limited.

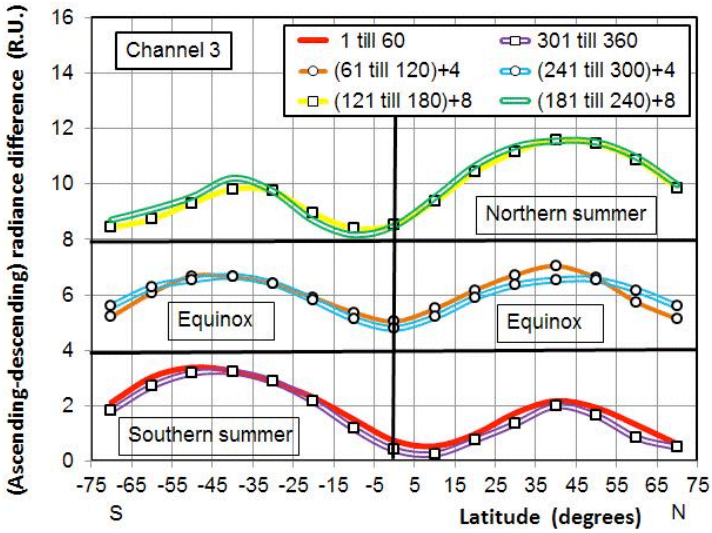

Figure 10. Ascending – descending orbit radiance difference as a function of latitude for channel 3 for different longitude bands. The ordinate has units of mW m^{-2} sr^{-1} cm^{-1}.

The amplitudes of the terdiurnal and quarter-diurnal temperature tides shown in Figures 9c and 9d are small and have considerable uncertainty because they depend strongly on the SSU radiance gradients between views 1 to 8 being correct. Tidal biases due to errors in this difference would probably be constant with latitude. Thus, the tides are present but the precise amplitude is open to question. The basic Hough mode for both tides would be similar and show a maximum in the tide near the equator. The comparison of the SSU terdiurnal tide with the measurements at 86 km from the microwave limb sounder divided by 8, (Forbes and Wu; 2006), shows similar variation with latitude.

5.2 The impact of solar tides on the time series analysis

In Figure 11, the spectroscopic differences have been eliminated as far as possible from comparisons between NOAA-9, NOAA-7 and NOAA-6, using the information contained in Figures 7 and 8 to provide a typical average difference. The differences primarily result from the semidiurnal tides, but the phase change in the tide between the northern and southern hemispheres, associated with the impact of the asymmetric (2,3) Hough function, seen in Table 6, means the variation with latitude of tidal differences in Figure 11 is not that similar to the variation with latitude of the semidiurnal tide in Figure 9. In Figure 12, the variation of the semidiurnal and quarter-diurnal tides during the day are plotted for channel 3 at 30°N and 30°S, with the bigger tidal difference occurring where the amplitude of the semidiurnal tide was smaller in the northern hemisphere.

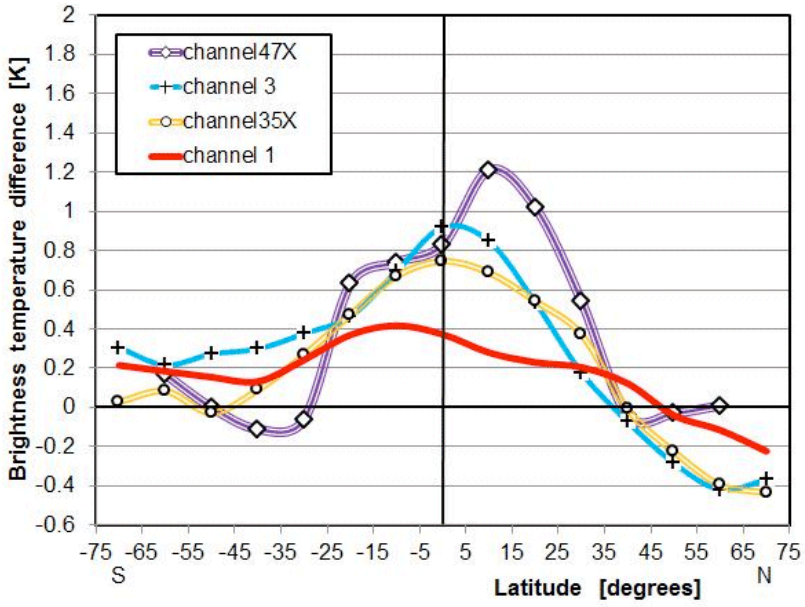

Figure 11. Typical tidal differences between observations at 15.00 local time and those at 19.30 local time.

The tidal difference between spacecraft varies with time of the year when the amplitude and phasing of the tides change, as can be seen for channels 35X, 3 and the uppermost channel 47X in Figure 13. The asymmetry in the tidal difference (15.00 - 19.30 LT) was towards the summer hemisphere, both in November/December/January/February and in May/June/July/August. However, purely in terms of global radiance difference, use of a single tidal compensation for the year will be accurate to about 0.1K for channel 3. Whilst the tidal differences in Figure 11 allow the early spacecraft measurements to be referenced to each other, they do not provide sufficient information on the phase and amplitude of the semidiurnal tides to ensure accurate correction of the orbit drift for NOAA-11 and NOAA-14. They can however be used as a reference between

observations at about 15.00LT and 19.30LT in the time series of both NOAA-11 and NOAA-14.

In the Met Office time series, the observations of all spacecraft were initially referenced to the observations at 19.30LT provided by NOAA-6. It was the most stable SSU of the early SSUs in terms of spectroscopic performance and was used as a reference observation up until the end of its operations in 1986. NOAA-6 observed at 19.30 LT and had to be linked to NOAA-9 observations close to 15.00 LT, using the values in Figure 11 together with any additional correction necessary for radiometric and spectroscopic differences between the two spacecraft. The tidal corrections applied by WANG for a change in orbit time from about 15.00 to 19.30 were lower than those used by the Met Office by about 0.1 K for each channel, see Table 10. Neither LIU or BRINDLEY made any corrections for tides.

The variation of global temperature observations for different local times of observation (see Figure 12) were combined to provide a plot of corrections for global brightness temperatures as a function of local time of observation, see Figure 14. For the two upper channels the correction necessary at the equator, was about twice that for the global radiance. If this correction is too small, an incorrect relationship between temperature changes at the equator and at high latitudes must follow in channels 2 and 3.

a

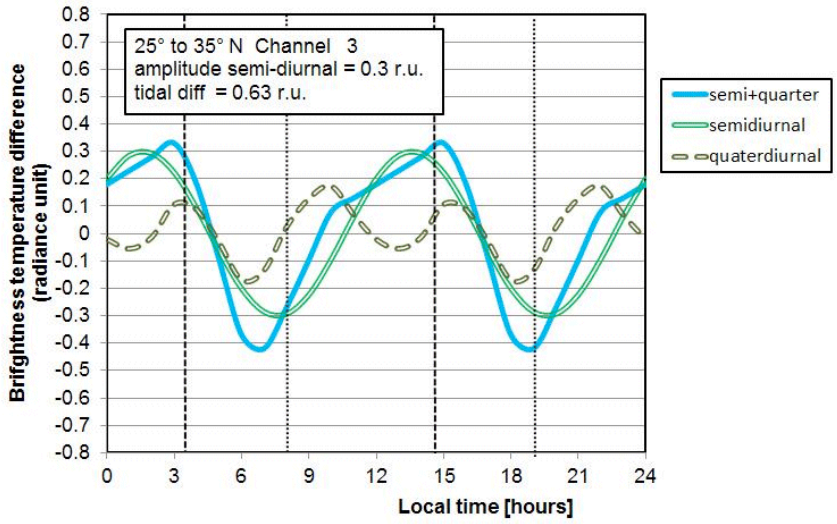

b

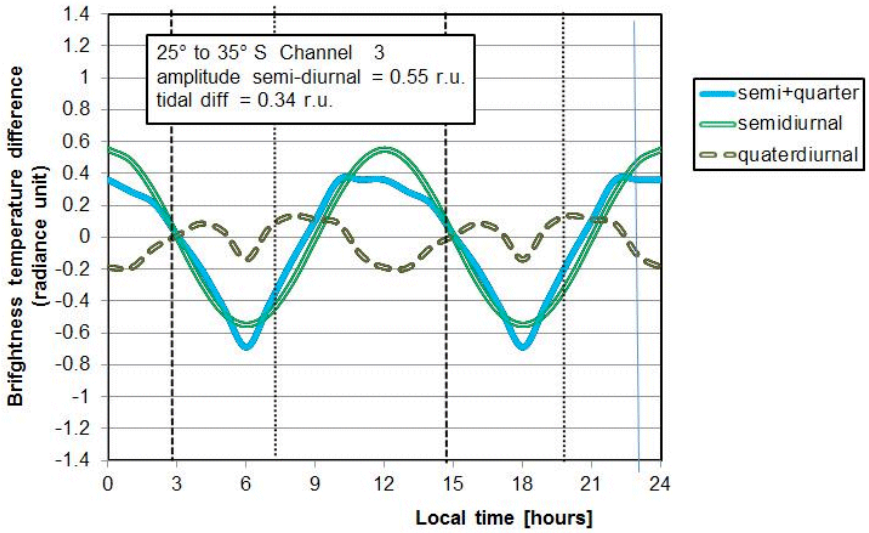

Figure 12 Variation of semidiurnal + quaterdiurnal tides with local time of day for channel 3 (a) 30°N and (b)30°S. Between dashed vertical lines NOAA-7 observations and between dotted vertical lines NOAA-6 observations.

NOAA-9 observations require a small correction for orbit drift because the difference between 14 and 16 LT cannot be ignored, but it is difficult to establish the precise phase of these semidiurnal tides. After this NOAA-11 orbit times drifted by a large amount, changing from 13:00 to 19:30 by early 1997. Thus, the NOAA-11 observations in 1997 must have the values shown in Figure 11 added to them to take account of the change in tides with orbit drift since 1989. Similarly NOAA-14 orbits drifted from 13:30 in 1995 to 19:30 in early 2004, so this time series also needs a similar adjustment to NOAA-11. After 1997, the NOAA-11 observation times drifted to 23:00 local time in 2004, and after 2004 NOAA-14 observing times drifted further to about 22:00 in local time in 2006. So by the end of NOAA-11 and NOAA-14 operations the correction for tides had become smaller.

SSU channel	Standard deviation of 6 month differences NOAA-14 and NOAA-11 compensated for changes in orbit times [K]	Uncertainty in systematic bias in NOAA-14 observations in 2005/6 [K]
47X	0.22	0.2
36X	0.27	0.2
3	0.18	0.1
2	0.16	0.1
26X	0.28	0.2
1	0.13	0.1
15X	0.14	0.1

Table 7. Comparison between 6 month SSU averages from NOAA-11 and NOAA-14 between 1997 and 2004, and an estimate of the uncertainty of systematic bias in NOAA-14 at the end of its life in 2006.

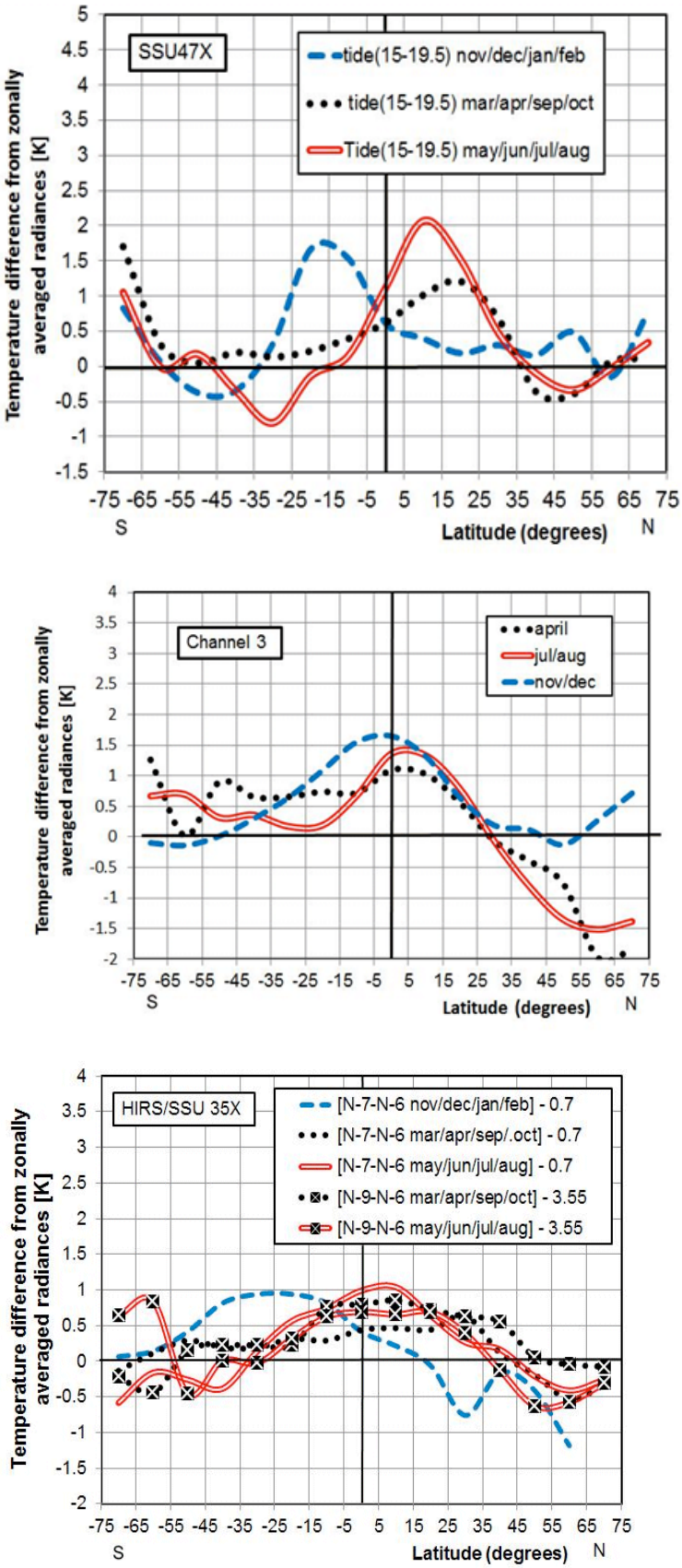

Figure 13 Tidal differences for different times in the year for channel 35X, 3 and 47X, derived from comparisons between NOAA-7 and NOAA-6 and NOAA-9 and NOAA-6 observing at 15.00 and 19.30 local time respectively(spectroscopic difference in NOAA-7 20 per cent higher than in NOAA-9 and of opposite sign).

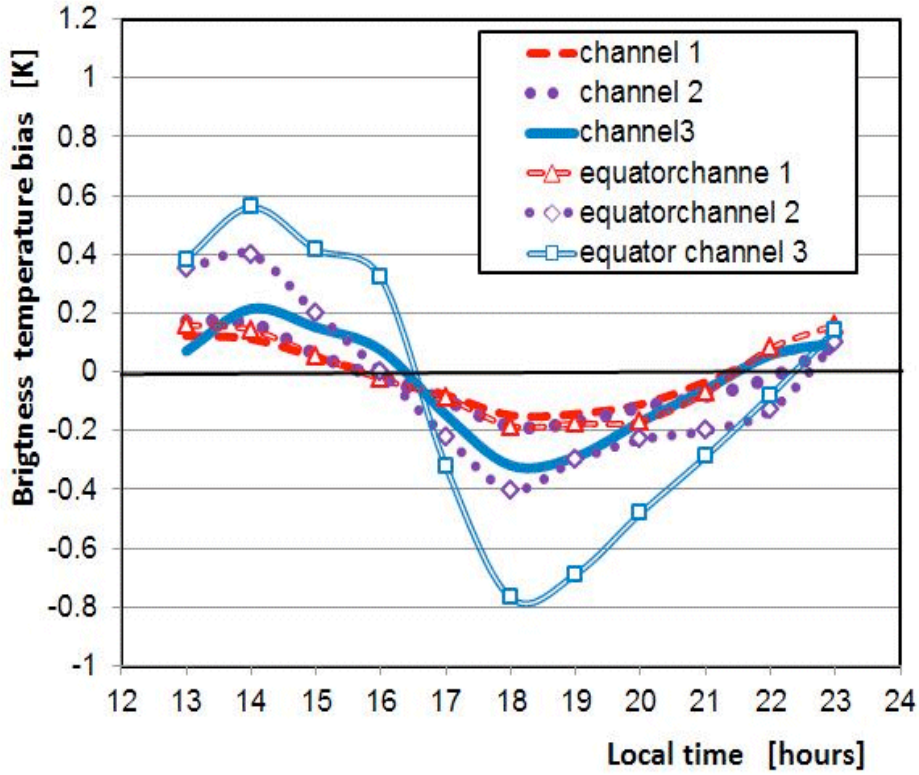

Figure 14. Variation of SSU global radiances (ascending and descending orbits averaged together) with local time of observation using information from equinox analysis, similar to that in Figure 12.

The effectiveness of the correction for tides on differences between NOAA-11 and NOAA-14 from 1997 until the end of 2003 can be seen in the standard deviation of the differences for 6 month periods, see Table 7. These are about 50 per cent higher than the values quoted for comparisons between early spacecraft in stable orbits in Tables 3 and 5. Tidal differences were very small in channel 15X, so this gives the best agreement between the two spacecraft. Corrections for channels 26X, 36X and 47X were the least reliable.

6. Time series analysis

6.1 Updated Met Office time series

In this paper, six month averages have been used to calculate the temperature differences from the long term average, with the differences then all referenced to produce a zero offset for the temperatures centred on the start of 1980.

The results for the three basic SSU channels are plotted in Figure 15(a). The changes of mean layer temperature with time in channels 1 and 2 are similar, but the changes with time are larger for channel 3, particularly between 1981 and 1997. The changes shown by these channels were cross-checked in 2006 by the NOAA Climate Prediction Center (A.J. Miller, personal communication) and were found to be reliable within the stated

uncertainties . The dates of the maxima and minima in the sunspot cycle are shown, and the time series for channel 3 shows evidence of a solar cycle in the brightness temperatures of amplitude about 0.3 K. The major volcanic eruptions are also indicated when significant step changes are seen in the temperature trends.

6.1.1 Channel 1 details

The time series between 1979 and the end of 1988, depends largely on the measurements of NOAA-6, unadjusted, plus interpolation from late 1986 onwards using NOAA-9. Note that NOAA-9 was not considered before late1986, because of problems with its radiances. The change in radiance measured by NOAA-6 was well defined, with more data from 1985 to 1986 in the Met Office real time data than is in the NOAA-CLASS archive. To match NOAA-6 to NOAA-9 requires a tidal adjustment increasing NOAA-6 global radiances by about 0.2K relative to TIROS-N, NOAA-7 and NOAA-9. In hindsight it is easier to reference to NOAA-7 orbit times as these were similar to the start of most of the succeeding SSU spacecraft orbits, but this does not change the outcome of the time series results shown here. The processing of NOAA-9 changed in March 1987 when the Met Office took over processing of radiances for this spacecraft. The values were matched to the preceding data from NOAA-9 so there was no discontinuity in the Met Office NOAA-9 global radiances at this time. In contrast, the NOAA-CLASS archive has a downward discontinuity in NOAA-9 in early 1987. Although NOAA-9 had a significant decrease in apparent cell pressure after 1987, comparison with NOAA-6 showed no significant trend, and it was assumed that any cell pressure change had been compensated by the drift in orbit observation time from 15.00 to 16.00 between 1987 and the end of 1988. An analysis of NOAA-CLASS data could be expected to give a slightly higher temperature fall by the end of 1988, because of the uncorrected change when some of the other instrumentation was switched off on NOAA-9 when it was no longer operational.

From 1989 until the end of 1996, the time series is mainly determined by NOAA-11 plus the early years of NOAA-14. The Met Office time series may not have had an adjustment for the change in cell pressure at the start of NOAA-11 operations. If this was the case, then the fall in temperature of the Met Office time series would need to be higher by 0.1K. The match between NOAA-9 and NOAA-11 is difficult with the raw CLASS archive data (C-Z. Zou, personal communication) having a downward trend immediately after launch, not seen in the WANG basic data. A tidal adjustment has to be made to NOAA-11 with at least 0.2K added to the measured radiances in 1994. It was unfortunate that NOAA-11 observations between 1995 and 1997 were not archived in the NOAA-CLASS

archive. Similarly NOAA-14 measurements require a tidal adjustment of about +0.2K in 2003-2005, with the tidal adjustment a little smaller at the end of NOAA-14 operation by 2007.

6.1.2 Channel 2 details

As with channel 1, TIROS-N and NOAA-6 channel 2 provide a time series of measurements with little need for PMC cell pressure adjustments, but a tidal adjustment between TIROS-N and NOAA-6 is required adding 0.3K to NOAA-6 radiances. NOAA-9, NOAA-11 and NOAA-14 have significantly different PMC cell pressures than NOAA-6 and TIROS-N, and were corrected as described earlier in section 4. The mixture of gases in the NOAA-7 PMC leak cannot be defined sufficiently to correct the pressure changes with the necessary precision required for climate studies. Thus the empirical study of tidal effects from the early SSUs had larger uncertainties in channel 2 than in channels 1 and 3. Tidal adjustments for orbit drift in NOAA-11 and NOAA-14 were slightly larger than those described for channel 1 above.

6.1.3 Channel 3 details

Although the tidal adjustments and PMC pressure cell adjustments are largest in channel 3, there is less controversy about the correct values for the time series analysis. The temperature trend over the SSU period is larger at these levels than in channels 1 and 2.

6.1.4 All upper level synthetic channels

The time series results for the upper channels, 47X, 36X, 3 and 2 are plotted in Figure 15(b). The results for 47X and 36X support the higher temperature drops seen in channel 3. At these levels the temperature mostly decreased with time from 1979 to 1998 (apart from the relative maximum associated in 36X and 3 with the sunspot cycle for a couple of years leading up to 1990) but became relatively stable after the sunspot minimum in 1996/7.

Unfortunately there was a break in the time series of SSU channel 2 observations in 1984 when NOAA-7 observations became unusable after NOAA-8 had failed and before NOAA-6 was turned on again in September 1984, see Table 8. Channel 35X brightness temperatures from NOAA-7 were used to reference NOAA-8 channel 2 measurements to NOAA-6 measurements in the Met Office analysis, when there was no channel 2 available on NOAA-7. Channels 2 and 35X peak at similar heights in the atmosphere (see Figure 16). The lack of channel 2 data in early 1984 was not critical for the time

series analysis, for channels 15X, 26X, 36X and 47X, as NOAA-6 was observing for most of late 1984 until late 1986, so there was a reliable link back to April 1983.

a

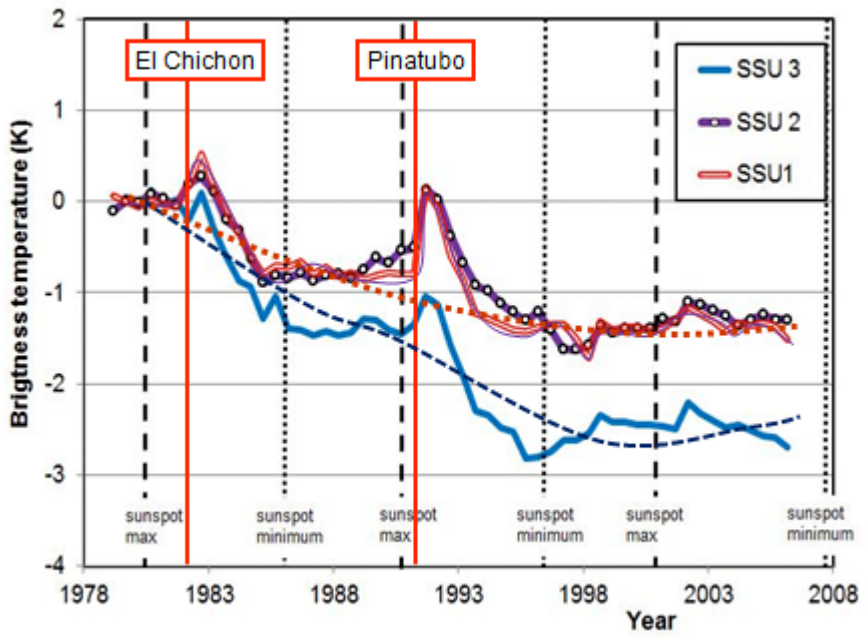

b

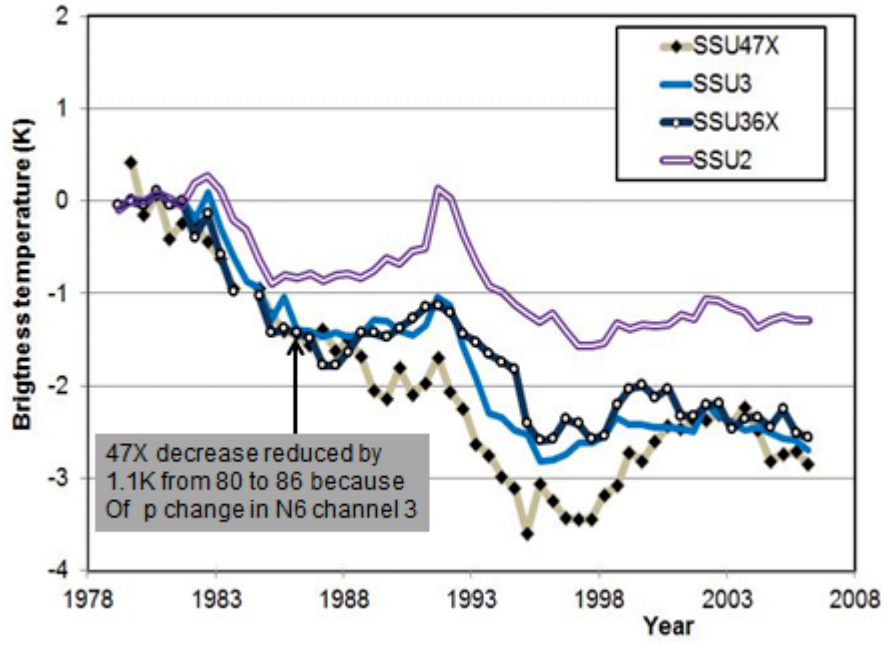

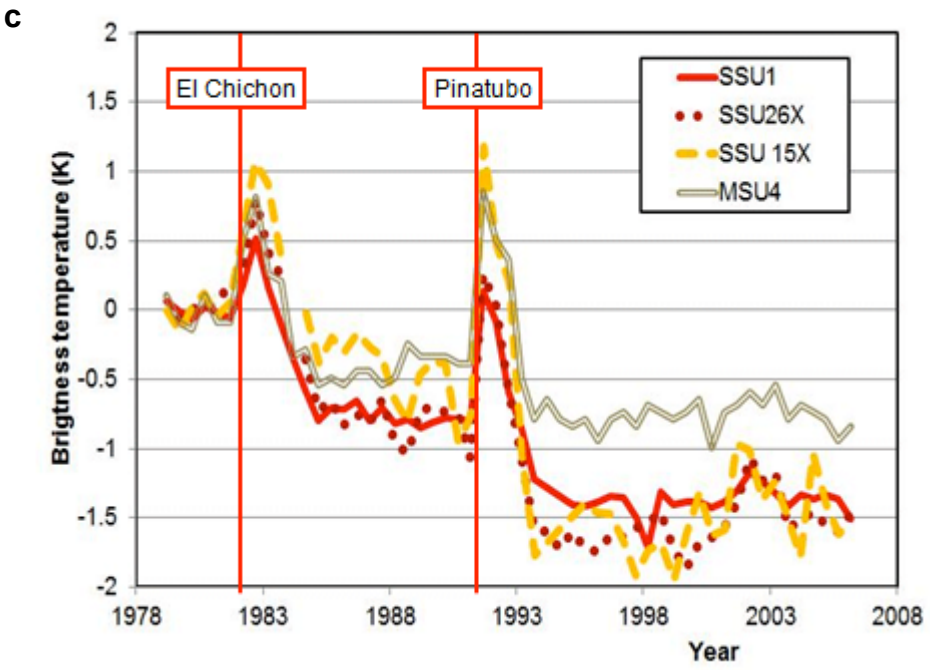

Figure 15. Time series of global (75°N to 75°S) temperature anomalies for 6 month averages for SSU channels 1 to 3, and 15X,26X,36X and 47X with temperature anomaly for each time series relative to 1979/1980. (a) basic channels,(b) all upper level channels) (c) all lower level channels + MSU 4 from Thompson et al (2012).

The comparison between 35X and channel 2 during this period suggests that channel 2 cell pressure corrections with time were unlikely to be in error by larger than 0.3K and so this supports the cell pressure change corrections for NOAA-9 and NOAA-11 used by the Met Office. However the Met Office time series analysis relies heavily on NOAA-6 radiometric and spectroscopic properties remaining stable after being turned on and off several times during this period.

6.1.5 All lower level synthetic channels

At lower levels the time series do not resemble a linear fall in temperature with time (see Figure 15b), but two periods with stable temperature interspersed with two local maxima in temperature caused by SO_2 and aerosol injected into the stratosphere by El Chichon in 1982 and Pinatubo in 1991. Both eruptions were followed by a drop in temperature within two years which resulted in lower temperatures than before. Channel 15X shows the largest temperature increase associated with El Chichon and Pinatubo. The channel 26X time series also suggests that the channel 1 time series is not in error by more than 0.4K.

6.1.6 Uncertainty estimates

Estimates of the uncertainties in the temperature trends are shown in Table 9 and the tidal correction is the main contribution for trends inferred from the SSU measurements.

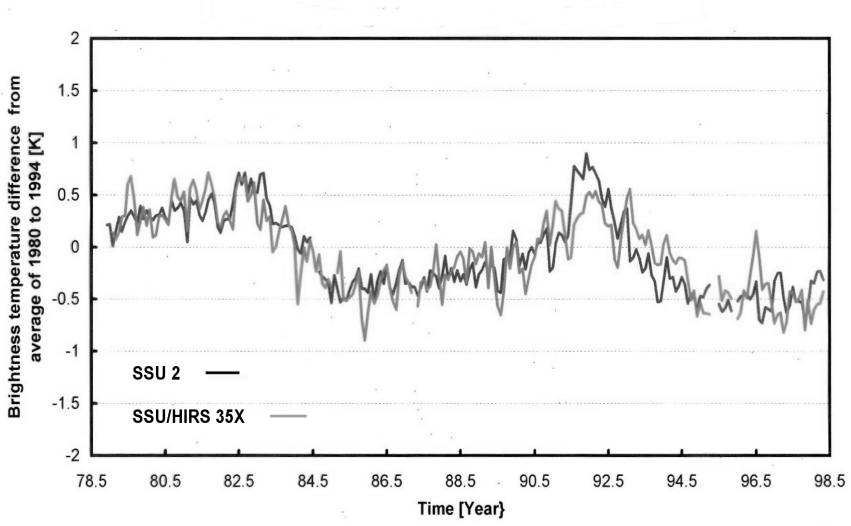

Figure 16. Comparison of global means for SSU channel 2 and HIRS/SSU channel 35X. Values between Mar 1983 and mid-1984 from NOAA-8 were matched to 35X values from NOAA-7 during this period. These data were used to check the time series analysis of SSU channel 2 before the correction required for increase in CO_2 in the atmosphere was applied to both channels.

Uncertainty in the correction for the increase of atmospheric CO_2 is higher for synthesised channels, given the higher probability of error in these weighting functions, and also for channel 3 where the exact position of the weighting function relative to the stratopause is critical for the correction required.

The temperature changes observed with the SSU from the Met Office and WANG published analyses are shown in Figure 17. The Met Office values differ a little from the previous published values in Thompson *et. al.* (2012), because the tidal correction of NOAA-11 and NOAA-14 between 1997 and 2006 has since been refined using a better representation of the semi-diurnal tides, as described in section 5, although the corrections applied for the tides are subject to considerable uncertainty. As a result the temperature trends for the Met Office analysis have been revised by -0.2K, -0.2K, and +0.4K in channels 1 to 3 respectively with uncertainties indicated in Figure 17. When the results are compared to the relevant model results in Thompson *et. al.* (2012), channels 1 and 3 are still close to the largest temperature drops found in any model, and the channel 2 temperature change is not as large as suggested by the models. The WANG values in Figure 17 correspond to Table 10 in their paper.

Spacecraft	Date	Amount of overlap	PMC pressure change at overlap	Influence of atmospheric tides	Limitation
TIROS-N – NOAA-6	1980-1981	At least 6 months		Tidal difference referenced to NOAA-6	TIROS-N channel 3 unusable
NOAA-6 – NOAA-9	1986-1987	At least 6 months	NOAA-9 Channel 1	Tidal difference referenced to NOAA-6. NOAA-9 tidal effects have small changes	
NOAA-9 – NOAA-11	1989-1990	At least 2 months	NOAA-11 Channels 1-3	NOAA-11, tidal effects change with time.	
NOAA-11 – NOAA-14	1995-2003	Many years	NOAA-14 Channels 2,3	NOAA-14 tidal effects change with time for both spacecraft	
*NOAA-7 – NOAA6	1982-1983	At least 9 months,	NOAA-7 Channel 3	Tidal difference referenced to NOAA-6	NOAA-7 channel 2 unreliable
*NOAA-7 – NOAA-8	1984-1985	At least 4 months	NOAA-8 Channel1	Tidal difference referenced to NOAA-8	NOAA-7 channel 2 unreliable

*Table 8. Overlaps crucial to the continuity of the SSU time series. [*NOAA-7 links NOAA-8 to NOAA-6, but as NOAA-6 was reactivated after NOAA-8 ceased operation, NOAA-7 and NOAA-8 are not so critical to the estimate of long term trends.]*

Channel	Total [K]	Tidal [K]	PMC p change [K]	Radiometric Matches [K]	Atmospheric CO_2 increase [K]
47X	0.76	0.47	0.5	0.25	0.2
36X	0.45	0.35	0.1	0.17	0.2
3	0.43	0.34	0.1	0.15	0.15
2	0.35	0.28	0.12	0.17	0.07
26X	0.49	0.38	0.08	0.23	0.2
1	0.28	0.22	0.07	0.14	0.07
15X	0.36	0.20	0.12	0.26	0.1

Table 9. Uncertainty (standard deviation) in the temperature change from 1980 to 2005 for all the SSU channels showing the relative importance of the uncertainty in the different adjustments.

The dot dash line in Figure 17 is an estimated temperature change profile with a vertical structure that matches the observed temperature changes to within ±0.5K, using the weighting functions in Figure 6. At pressures lower than 30 hPa this temperature change profile has been limited to layers about 8 km thick. The difference between the observed temperature changes by channels 2 and 3 cannot be exactly matched using any reasonable profile of temperature change with the weighting functions in Figure 6. However considering the uncertainties associated with each layer mean temperature realistic profiles are possible. In Figure 17 the same temperature change has been assumed between 30 and 3 hPa, and then a sudden increase to a different change

between 3 and 0.3 hPa. Higher resolution in the temperature changes at pressures lower than 3 hPa, cannot be seen by the SSU measurements, although the mean temperature change up to 0.3 hPa has to be significantly larger than from 30 to 3 hPa. The large uncertainty in the 47X temperature change plus the uncertainty in the observed radiances in this channel limit what can be deduced in the lower mesosphere from the SSU, and any improved estimate would need to know the temperature changes at pressures lower than 0.3 hPa, which are not available.

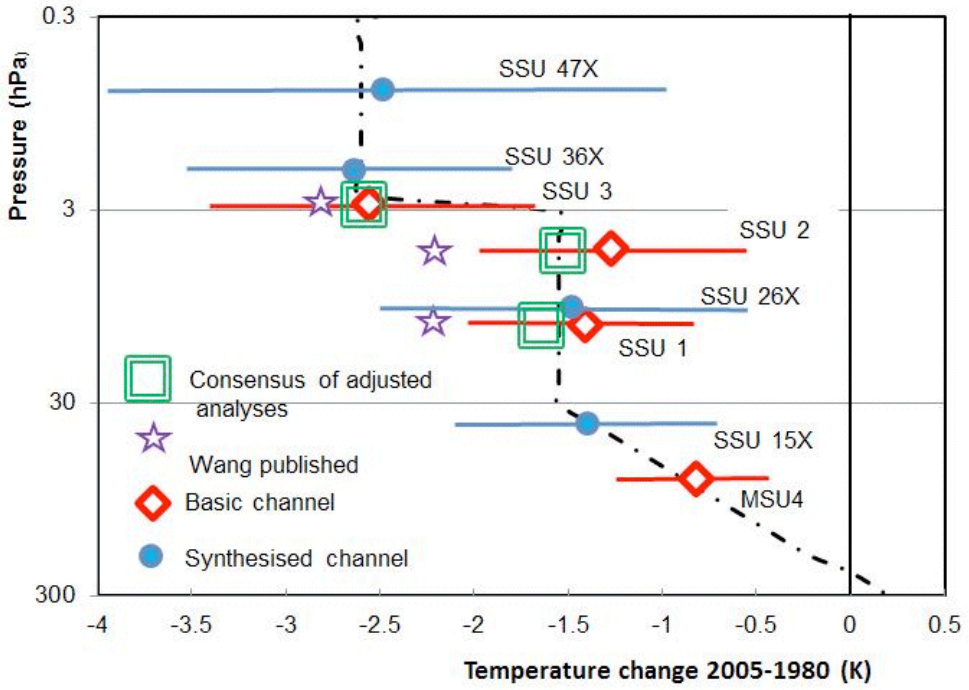

Figure 17. Change in global brightness temperature measured by the SSU between 1980 and 2005. The dot dashed line is a temperature change profile that reproduces the changes to near the uncertainty limits, using the weighting functions in section 4.2 with the radiosonde changes reported in Thompson et al (2005) at the lowest levels. "Wang published" is the temperature change found in the final WANG time series (see Figure 15, WANG). The consensus of adjusted analyses come from the data in Tables 10 and 11 in this paper. The uncertainties shown by the horizontal error bars are for twice the standard deviations.

Details of the weighting function computations (width of the weighting functions) could be subject to error, and this would then result in increased uncertainty in the details of the synthesised channel weighting functions. However, there is no doubt that basic and synthesised channel temperatures are centred close to the levels indicated in Figure 17.

6.2 Analysis of the differences between the Met Office time series and others

In Table 10, three time periods are used to check the temperature trends in the Met Office, WANG, LIU, BRINDLEY and NASH analyses. WANG published a time series for the SSU observations after their final merging process and the results from these are shown in Figure 17. In Table 10 WANG data come from their published time series and

also before merging was applied, LIU and BRINDLEY for this study were also modified, see Tables 10 and 11.

6.2.1 Modifications to the WANG, LIU and BRINDLEY and NASH time series

In Table 10, the data used for our "consensus" values are in the greyed columns. The adjusted values for WANG in Table 10 are the temperature changes from the unmerged time series in WANG (after tidal correction was applied) as shown in Table 10 plus the additional tidal correction for WANG to make the adjustments similar to those of the Met Office empirical adjustment model. The "WANG adjusted" values are then close to the Met Office trends for channel 1 and higher for channel 2 see Table 10.

LIU corrected the data series for individual satellite PMC cell pressure changes, the increase of atmospheric carbon dioxide, but came to the erroneous conclusion that tidal effects were negligible. So the LIU (adjusted values) have had the Met Office empirical tidal correction applied for NOAA-6, NOAA-11 and NOAA-14.The LIU time series have no information between the end of NOAA-8 observations in early 1984 and the beginning of NOAA-9 observations in1985, because NOAA-7 and NOAA-6 observations after 1984 were not used. For this study, the link between NOAA-6/NOAA-8 and NOAA-9, was provided by the consensus from the Met Office and WANG temperature changes from 1983 to 1985.

BRINDLEY(adjusted) has had a correction for the increase in atmospheric CO_2 added according to the values in Shine *et.al.* (2009) and tidal correction as implemented for LIU. Although the BRINDLEY basic data came from the Met Office, they provide good evidence that no special adjustment procedures were being applied to NOAA data by the Met Office. Whilst it might be expected that comparing data from the different sources would show that large errors in basic radiances caused the differences in the results, this is not the case, but the differences result from the addition of several small sources of error as described in the following sub-sections.

Table 11 shows the consensus values obtained from the various greyed analyses in Table 10, i.e. analyses with similar tidal adjustments, and all corrections applied. As can be seen in Figure 17 the Met Office values generally sit close to the consensus, within the uncertainties attributed to the analyses. From these data it seems safe to conclude that the temperature drop in channel 3 was about 0.4 K higher than in channels 1 and 2 for both 1979-88 and 1989-1996, but less than 0.2 K higher between 1997 and 2006.

Channel 1	1979-1988	1989-1996	1997-2006
Met Office(revised)	-0.8	-0.6	0
Brindley et al, tidal + atmospheric CO_2 corrections	-0.85	-0.85	
LIU adj for empirical tide + revised spacecraft matches	-08	-0.8	0
Wang et al,published	-1.1	-1	-0.2
Wang without merging	-0.8	-0.8	-0.15
Wang adjust for empirical tide	-0.8	-0.7	-0.1
NASH+Met Office cell pressure adj +empirical tide	-0.95	-0.8	-0.1
Consensus	-0.85	-0.75	-0.05

Channel 2	1979-1988	1989-1996	1997-2006
Met Office(revised)	-0.85	-0.6	0.1
LIU adj for empirical tide + revised specacraft matches	-0.75	-0.7	0.2
Wang et al published	-1.1	-1	-0.3
Wang without merging	-1.1	-0.85	-0
Wang adjust for empirical tide	-1.1	-0.7	0.1
NASH+Met Office cell pressure adj +empirical tide	-1.1	-0.75*	0.10
Consensus	-1	-0.7	0.1

Channel 3	1979-1988	1989-1996	1997-2006
Met Office (revised)	-1.4	-1.2	+0.05
Wang et al published	-1.2	-1.5	-0.2
Wang without merging	-1.2	-1.1	-0.3
Wang adjust for empirical tide	-1.2	-1	-0.2
NASH +Met Office cell pressure adj +empirical tide	-1.3	-1.3	-0.2
Consensus	-1.3	-1.2	-0.1

Table 10. Summary of differences between Met Office, WANG, LIU, BRINDLEY and NASH time series analysis for basic SSU channels. . Greyed values used in consensus estimates.

	MSU 4	Channel1	Channel 2	Channel 3
1979-88	-0.45 ±0.05	-0.84 ±0.1	-0.95 ±0.3	-1.3 ±0.2
1989-96	-0.50 ±0.1	-0.75 ±0.2	-0.69 ±0.1	-1.17 ±0.3
1997-2006	0.1 ±0.15	-0.05. ±0.1	0.13 ±0.1	-0.12 ±0.3
Total	-0.85 ±0.15	-1.64 ±0.2	-1.5 ±0.2	-2.6±0.1

Table 11. Summary of adjusted results for the temperature trends from 1980 until 2005 from Met Office, WANG, LIU ,BRINDLEY and NASH showing the consensus and the range of the values found in terms of the ± value.

6.2.2 Data coverage

The analysis techniques used by WANG were different from those described here for the Met Office. WANG used all SSU fields of view and hence covered a wider latitude range than the Met Office. The limb-brightening of SSU views 1 and 8 is readily computed directly from the SSU measurements and the values found were larger than the values found in simulations by WANG, e.g. see typical example in Brownscombe *et. al.* (1985). Only nadir views were used for the Met Office monitoring, accepting that reliable zonal averages would not be obtained at higher latitudes than 75° as limb-brightening varied a great deal from year to year at the highest latitudes, and these variations were not well simulated in numerical models. For example Kobayashi *et. al.* (2009) mitigated inter-spacecraft differences but could not eliminate all the differences at high latitudes. However comparison of the WANG time series of radiances from individual spacecraft with the Met Office time series indicates that the difference in areal coverage was not a major cause of discrepancies. The coverage of LIU is not reported in their paper and BRINDLEY used up to 70° latitude. The Met Office used data supplied directly from NOAA with no additional processing apart from averaging into latitude bands for individual nadir views as stated in Pick and Brownscombe (1981), Nash and Forrester (1986) and Nash (1988).

6.2.3 Data availability

WANG states that the SSU data were mainly acquired from the NOAA CLASS system suggesting that some of their data came from other sources, which would most likely be during periods when SSU data was coming from a spacecraft that had lost its operational status. LIU did not use NOAA-6 or NOAA-7 observations after 1983. WANG used NOAA-7 channel 2 observations in 1984 when they were not valid.

When data reception was incomplete, the Met Office was very careful to eliminate 5 day periods where reliable zonal averages could not be obtained at all latitude bands. BRINDLEY describes how this was corrected for with NOAA-6 and NOAA-9. These two

spacecraft were critical for defining the temperature change between 1979 and 1988, so even small differences in the data availability for these spacecraft between 1984 and 1989 may have led to temperature changes different from those found in the Met Office analysis. There is a temperature drop/discontinuity in the time series of WANG/LIU NOAA-9 data in channel 1 and channel 2 in early 1987 when NOAA-9 lost operational status. This temperature drop is not present in the Met Office, or BRINDLEY time series. The Met Office processing for NOAA-9 changed at this time, but great care was taken to ensure no discontinuity in the time series when NOAA-9 lost operational status. Hence the radiance drops in the WANG and LIU data at this time were caused by an uncorrected step change in NOAA-9 radiances coincident with the NOAA-9 change in operational status. This increased the temperature fall between 1986 and 1989 by up to 0.2 K in both channels. Note that WANG and LIU data have not been corrected for this in Table 10.

WANG NOAA-11 data between 1997 and 2000 in channels 1 and 2 have lower radiances than the data in 1994, but this was not the case for NOAA-11 data supplied to the Met Office from NOAA between 1989 and 2003. These NOAA-11 data (used in the Met Office time series) were more extensive in temporal coverage than that used by WANG.

The availability of NOAA-6 data after 1983 varies a great deal between analyses, and these values are quite critical for underpinning the temperature changes that occurred between 1979 and 1989. Nash and Edge (1989) state that NOAA-6 observations were available in the Met Office from September 1984 until June 1985 and then from November 1985 until October 1986, and comparison data from the periods up to early 1986 were reported for 25°N to 25°S in Nash and Forrester (1986). NOAA-6 data from March 1986 until October 1986 were used in generating the difference plots in Figure 4, so Met Office NOAA-6 data coverage during this period was sufficient to get reliable monthly computations of synthesised radiances. WANG had no NOAA-6 data in 1984 and only a very short fragment in early 1985. NOAA-6 WANG data started again in October 1985, but missed most of the data in mid-1986.

It appears that some differences in the time series trends arise from differences in matching NOAA-9 observations with NOAA-6 in 1985/7, and the join between NOAA-11 and NOAA-14 in 1995/6, partly associated with the different data coverage in these periods.

6.2.4 Differences in radiometric quality

The omission of the space view anomaly correction from the early data in the CLASS archive led to significant scatter in the WANG unmerged time series between 1979 and 1988 for channels 1 and 2, but not for channel 3. The WANG merging process in channel 1 increased the temperature change between 1989 and the end of 1996 by 0.3K, because it mismatched NOAA-6 to NOAA-9 and NOAA-11 relative to NOAA-14. For channel 2 the WANG merging fits the data better, but doesn't increase NOAA-14 to match NOAA-11 in 1995. This was also the case in channel 3.

6.2.5 Differences in spectroscopic corrections

There were differences in spectroscopic corrections applied, but these were not large, given that the methods used were quite different. The corrections for limb-brightening used by the Met Office agreed with the corrections computed from transmission models of the atmosphere which indicates that this was not a major source of discrepancies in the analyses for channels 1 and 3. There were more significant differences for channel 2. The anomalous NOAA-7 channel 2, where the composition of the leak was complex, could not be corrected reliably enough for use in a time series analysis.

6.2.6 Differences in tidal corrections

In this paper, the tides were inferred directly from SSU measurements and not by comparison with reanalysis fields. The semidiurnal and quaterdiurnal tides largely control the variation of the average of ascending and descending orbits with local time, as shown in Figure 14. The time series of inter-spacecraft differences for channel 1 from 1980 until 1985 in Nash and Forrester (1986) showed little variation in the tidal difference with time of year in the tropics. For channel 1 the values used were derived from inter-spacecraft differences over many years, so the uncertainty in the amplitude was about 0.03K in 0.2K, and the overall tidal corrections used by the Met Office are unlikely to have an uncertainty larger than 0.05K, see Table 9.

For channel 2 Brownscombe and Pick (1981) found a typical difference between TIROS-N and NOAA-6 in global brightness temperatures of 0.4K. Typical inter-spacecraft differences near the equator were about 0.6 to 0.7K for TIROS-N – NOAA-6 and also NOAA-9 – NOAA-6, (once the NOAA-9 radiance error was corrected), see Nash and Forrester (1986). In the Met Office adjustments in this paper, a global temperature difference of about 0.32 K for the difference between observations at 15:00 and 19:30 local time was used.

With channel 3, the spectroscopic differences increased very rapidly after 1982 as shown in Nash and Forrester (1986), but there was a peak in the inter-spacecraft differences between 25°N and 25°S centred at the beginning of each year. The tidal estimates in Figure 13 for channel 3 where the spectroscopic differences have been corrected, show that in November/December the effect of the tides on inter-spacecraft differences gave a higher difference than at other times of the year in the tropics. For channel 3 the global tidal difference between 15.00 and 19.30 LT used in the corrections here was about 0.42 K, and the tidal corrections are unlikely to have an uncertainty larger than 0.15K.

7. Conclusions

The Met Office provided the SSU instrument to monitor stratospheric temperatures as part of its contribution to the Global Observing System from 1978 until 2006. It has monitored the instrument performance throughout the period of operation providing feedback to NOAA. In particular, care was taken to ensure data from satellites that had lost operational status, because of other instrument failures on the same platform, were of the same radiometric quality as the operational data received from NOAA in real time. Space view anomaly corrections were supplied to NOAA before the launch of each instrument and users were informed of the status of the PMC pressure variations once in orbit.

The SSU was not designed to provide climate quality measurements of stratospheric temperature but with careful reprocessing, as described in this paper, temperature trends can be inferred from the measurements. There are several factors affecting the time series of stratospheric temperatures inferred from the SSU. For example the archiving of the SSU data when a spacecraft had lost operational status was very variable, and this becomes important when deriving temperature trends as SSUs were not launched on every spacecraft due to the limited numbers of instruments available.

Several independent groups, in addition to the Met Office, have analysed the complete SSU time series and the consensus values of temperature trends from 1980 until 2005 in Table 10 are very close to the Met Office results presented in this paper given the uncertainties quoted in Table 9. Explanations are provided for many of the differences between the temperature trends published by WANG for this period for channels 1 and 2. The changes in temperature obtained, both for global temperatures and for the variation with latitude shown in Thompson et al (2012), do not have large unidentified errors outside the uncertainties quoted in Table 9 of this paper.

Three synthesised channels provide an additional source of information that can corroborate the changes seen by the basic channels. These used limb-brightening measurements from other basic channels. SSU channel 26X and 36X time series results were similar to channels 1 and 3. Channel 15X results are from pressure levels intermediate between MSU 4 and SSU 1 and the temperature changes were intermediate between the temperature falls found in MSU 4 and SSU 1, see Figures 15 and 17. In Plate 1 of Ramaswamy *et. al.* (2001) the variation of trend with latitude for channel 15X is shown. These values were not corrected for the increase in atmospheric carbon dioxide. If the correction is applied the effect would be to *increase* the downward trends, especially in the tropics, reducing the anomalous heating in the tropics (as found in some SPARC working documents in 2006), so there is some confidence in the validity of these measurements, given there is increased uncertainty compared to the basic channels. Channel 47X results show a higher temperature drop between 1979 and 1995 than the other upper channels, but overall temperature change throughout the whole period was similar to channels 3 and 36X, indicating that the layer of highest temperature fall near the stratopause extended up to about 0.5 hPa. However, the uncertainty in this result is probably approaching 1 K taking into account the difference in weighting functions between the equator and high latitudes.

Recently a study of the differences between the measured and simulated SSU radiances using the ERA-Interim reanalysis, along with all other observations, has been undertaken by Simmons *et. al.* (2013). The reanalysis includes some radiosondes which ascended above 10hPa. The SSU data used in the ERA-40 and ERA-Interim reanalyses were taken from both the real time data stream from NOAA and various other centres to complete any gaps in coverage. The short periods of rapidly changing differences seen for some channels of the SSU compared to the ERA-Interim reanalysis are all explained either by changes in PMC cell pressures as shown in Figure 7 or due to an incorrect calibration (e.g. space view correction for pre-1980 TIROS-N data). This gives further confidence the differences in the SSU radiance record reported by several authors can be explained by the factors reported in this paper.

8. Acknowledgements

The authors would like to acknowledge the large team of Met Office engineers and scientists who contributed to the building and deployment of the SSU, including K. Stewart, D.E. Miller, J.L. Brownscombe, D.R. Pick, B. Barwell, G.P Carruthers, B. Tonkinson, P. Evans, S. Stringer, E. Hibbett, D. Warner and those who helped in the long term monitoring of the SSU including, G. Forrester, P.R. Edge, T.J. Oakley, M. Bailey, M. Turp and at NOAA Climate Prediction Center, A.J. Miller and R. Lin. The weighting functions computations were produced by J. Barnett (University of Oxford) and made available to the authors through K. Shine (University of Reading).

Bibliography

Alexander, J. and Barnet, C (2007) Using Satellite Observations to constrain parameterizations of Gravity wave Effects for Global Models. *J. Atmos. Sci,* **64**, 1652-1665.

Bailey, M.J., O'Neill, A., and Pope, V.D. (1993) Stratospheric Analyses Produced by the United Kingdom Meteorological Office. *J. Appl.Met*.,**32,** 1472-1483

Brindley, H.E., Geer, A.J. and Harries, J.E. (1999), Climate variability and trends in SSU radiances: A comparison of model predictions and satellite observations in the middle stratosphere. *J. Clim*, **12**, 3197-3219

Brownscombe, J.L., Nash, J., Vaughan, G and Rogers, C.F. (1985) Solar tides in the middle atmosphere. I: Description of satellite observations and comparison with theoretical calculations at equinox. *Quart. J. R. Met. Soc*., **111,** 677-689

Chen, Y., Weng, F., Han, Y. and Liu, Q. (2008), Validation of the Community Radiative Transfer Model by using CloudSat data, *J. Geophys. Res*., **113**, D00A03, doi:10.1029/2007JD009561.

Curtis,P.D, Houghton,J.T., Peskett,G.D. and Rodgers,C.D. (1974) Remote sounding of atmospheric temperature from satellites. V The Pressure Modulator radiometer for Nimbus F.. *Proc. R. Soc. Lond*. **A.337**, 135-150

Ellis ,P., Holah,G.,Houghton,J.T., Jones T.S.,Peckham,G.,Peskett,G.D., Pick, D.R., Rodgers, C.D., Roscoe, H., Sandwell, R., Smith, S.D. and Williamson, E.J. (1973). Remote sounding of atmospheric temperature from satellites IV. The selective chopper radiometer for Nimbus 5. *Proc. R. Soc. Lond*. **A.334**, 149-170

Fleming, E. L., S. Chandra, J. J. Barnett, M. Corney, (1990) Zonal mean temperature, pressure, zonal wind and geopotential height as functions of latitude, *Adv. Space. Res.,* **10***,* 11–59

Forbes, J. M., and Wu, D. (2006) Solar tides as revealed by measurements of Mesosphere temperature by the MLS experiment on UARS . *J. Atmos . Sci.* **63,** 1776-1797

Healey,S.B., Eyre, J.R., Hamrud, M. and Thépaut. J.N. (2007) Assimilating GPS radio occultation measurements with two dimensional bending angle operators. *Q.J.R. Met. Soc,* **133,** 1213 – 1227

Houghton ,J.T. and Smith, S.D. (1970) Remote sounding of atmospheric temperature from satellites. I Introduction. *Proc. R. Soc. Lond*. **A.320**, 23-33

Kobayashi, S., Matricardi, M., Dee, D. and Uppala, S.(2009) Towards a consistent reanalysis of the upper stratosphere based on radiance measurements from SSU and AMSU-A. *Quart. J. R. Met. Soc*., **1351,** 2086-2099

Lauritson, L., G. J. Nelson, F. W. Porto. (1979). Data extraction and calibration of TIROS-N/NOAA radiometers. NOAA Technical Memorandum NESS-107. National Environmental Satellite Service, Washington, D.C.

Liu, Q. and Weng, F. (2009) Recent Stratospheric Temperature Observed from Satellite Measurements. *SOLA,* **5***, 053 056, doi:10.2151/sola.2009 014*

Nash, J. and Brownscombe, J.L. (1982) Validation of the Stratospheric Sounding Unit. *Adv. Space. Res.* **2**, *No.6,* 59-62

Nash, J. (1988) Extension of explicit radiance observations by the Stratospheric Sounding Unit into the lower stratosphere and lower mesosphere. *Quart. J. R. Met. Soc.*,**114,** 1153-1171

Nash, J. and Edge, P.R, (1989) Temperature changes in the stratosphere and lower mesosphere 1979-1988 inferred from TOVS radiance observations. *Adv. Space. Res* Vol. **9**, 333-341

Nash, J. and Forrester, G.F.(1986) Long-term monitoring of stratospheric temperature trends using radiance measurements obtained by the TIROS-N series of NOAA spacecraft. *Adv. Space. Res* Vol. **10**, 37-44

Nash.J., Smout, R., Oakley, T., Pathack,B. and Kurnosenko, S. (2006). Limitations on radiosonde sampling caused by small scale atmospheric motions, Section 11.4, WMO Intercomparison of Radiosonde Systems, Vacoas, Mauritius, 2-25 February 2005. *I.O.M. Report No.*83, *WMOT/D1303*

Pick ,D.R and Brownscombe, J.L. (1981) Early results based on the Stratospheric channels of TOVS on the TIROS-N series of operational satellites. *Adv. Space. Res* Vol. **1**, 247-260

Ramaswamy, V., et al. (2001) Stratospheric Temperature trends: Observations and model simulations. *Rev. Geophys.*,***39,*** 71-122

Randel, W. J. et al. (2009) An update of observed stratospheric temperature trends. *J. Geophys. Res*. **114,** D02107 1-21

Saunders R.W., Hocking, J., Rundle, D., Rayer, P., Matricardi, M., Geer, A., Lupu, C., Brunel, P., Vidot,J. (2013) RTTOV-11 science and validation report. NWP SAF Report, http://research.metoffice.gov.uk/research/interproj/nwpsaf/rtm/docs_rttov11/rttov11_svr.pdf

Seidel,D.J., Free,M. and Wang, J. (2005) Diurnal cycle of upper air temperature estimated from radiosondes. *J. Geophys. Res*., **110,** D09102,doi:10.1029/2004JD005526 1-13,

Seidel,D.J., Gillett,N.P., Lanzante,J.R, Shine, K.P. and Thorne, P.W. (2011) Stratospheric temperature trends: our evolving understanding. *Wiley Interdisc. Rev. Clim. Change,* **2,** 592-616

Shine,K.P, Barnett,J.J. and Randel, W.J.(2008) Temperature trends derived from Stratospheric Sounding Unit radiances: the effect of increasing CO_2 on the weighting function. *Geophys. Res. Lett*, **35**, L02710, 1-5

Simmons, A.J., P.Poli, D.P.Dee, P. Berrisford, H. Hersbach and C. Puebey. (2013) Estimating low frequency variability and trends in atmospheric temperature from the ERA-Interim reanalysis. *Q.J.R. Meteorol. Soc. (in press)*

Thompson, D.W. and Solomon, S. (2005) Recent stratospheric climate trends as evidenced in radiosonde data:global structure and tropopsheric linkages. *J. Clim* **18** 4785-4795

Thompson, D. W. J., D. J. Seidel, W. J. Randel, C.-Z. Zou, A.H. Butler, C. Mears, A. Osso, C. Long, R. Lin, (2012) The mystery of recent stratospheric temperature trends. *Nature,* **491**, 692-697. *doi:10.1038/nature11579*

Uppala, S. M., KÅllberg, P. W., Simmons, A. J., Andrae, U., Bechtold, V. D. C., Fiorino, M., Gibson, J. K., Haseler, J., Hernandez, A., Kelly, G. A., Li, X., Onogi, K., Saarinen, S., Sokka, N., Allan, R. P., Andersson, E., Arpe, K., Balmaseda, M. A., Beljaars, A. C. M., Berg, L. V. D., Bidlot, J., Bormann, N., Caires, S., Chevallier, F., Dethof, A., Dragosavac, M., Fisher, M., Fuentes, M., Hagemann, S., Hólm, E., Hoskins, B. J., Isaksen, L., Janssen, P. A. E. M., Jenne, R., Mcnally, A. P., Mahfouf, J.-F., Morcrette, J.-J., Rayner, N. A., Saunders, R. W., Simon, P., Sterl, A., Trenberth, K. E., Untch, A., Vasiljevic, D., Viterbo, P. and Woollen, J. (2005), The ERA-40 re-analysis. *Q.J.R. Meteorol. Soc.,* **131***:* 2961–3012. *doi: 10.1256/qj.04.176*

Wang, L., Zou, C.-Z. and Qian, H. (2012) Construction of stratospheric temperature data records from stratospheric sounding units. *J. Clim.* **25**, 2931–2946

Wentz, F.J. and Schabel, M. (1998) Effects of orbital decay on satellite derived lower tropospheric temperature trends, *Nature, **394,*** 661-664

WMO (2008) Measurements of upper air pressure, temperature humidity. *Chapter 12, WMO Guide to Meteorological Instruments and Methods of Observation*, *WMO No-8*

Wu, D. L. and Waters, J.W. (1996) Gravity-wave-scale temperature fluctuations seen by the UARS MLS, *Geophys. Res. Lett.*, **23**, 3289-3292

Yan, B. and Weng F. (2012) Assimilation of F-16 Special Sensor Microwave Imager/Sounder Data in the NCEP Global Forecast System. *Wea. Forecasting*, **27**, 700–714. doi: http://dx.doi.org/10.1175/WAF-D-11-00062.1

Zou,C.-Z. and Wang, W. (2010). Stability of the MSU-derived atmospheric temperature trend. *J. Atmos. Oceanic Technol.,***27***,1960-1971*

Annex 1. Timeline of SSU data

Space-craft	*Data available*	*SSU channel used*	*SSU Status*	*Comments*
TIROS-N	Dec 78- July 80	1,2	Operational	Channel 3 very noisy , systematic bias unstable
NOAA-6	Dec 79 – April 83 Sept 84 - June 85 Nov 85- Oct. 86	1,2,3	Operational *SSU collected *SSU collected	No HIRS-2 after April 1983
NOAA-7	Jan. 82 - July 83 Aug 83 – Feb 85	1,2,3 1,3	Operational *SSU collected	Self calibration of channel 2 not valid after July 1983
NOAA-8	May 83 - Jun84 Jul 85 – Sept 85	1,2,3 2,3	Operational *SSU collected	Channel 1 very noisy in 1985, because of pickup of 3rd harmonic from PMC 3
NOAA-9	Mar 85 - Feb 87 Mar 87 – Jan 89	1,2,3	Operational *SSU collected	Data from Oct 1988 onwards not retained in archive.
NOAA-11	Oct 88- Jan 95 Feb-95 – Nov03	1,2,3	Operational *SSU collected	Small data gap in UK time series archive in May1995
NOAA-14	Feb 95- Jan 00 Feb 00 – Jan 06	1,2,3	Operational *SSU collected	Small data gap in UK archive in time series May 1995

*SSU still transmitting and being received by NOAA at lower priority than operational, in some cases data were processed at NOAA by the usual software and in a limited number of cases the raw data were transmitted to the Met Office for processing.

Table 1. SSU instruments producing useful information for the time series of atmospheric brightness temperatures. The SSU on NOAA-14 was the 1990's rebuild of the development model, originally completed in 1976. Otherwise most SSUs were completed and stored in suitable dry storage cases by the end of 1980. [Two other SSUs were launched on NOAA-B and NOAA-13, but these spacecraft did not achieve or remain in a viable orbit.]

Met Office
FitzRoy Road, Exeter
Devon EX1 3PB
United Kingdom

Tel (UK): 0870 900 0100 (Int) : +44 1392 885680
Fax (UK): 0870 900 5050 (Int) :+44 1392 885681
enquiries@metoffice.gov.uk
www.metoffice.gov.uk